Aus dem Department für Diagnostische Labormedizin der Universität Tübingen

Institut für Medizinische Mikrobiologie und Hygiene

Sektion Zelluläre und Molekulare Mikrobiologie

# Investigating the effect of the HilD inhibitor C26 on *Salmonella* pathogenicity mediated by the giant adhesin SiiE encoded on *Salmonella* pathogenicity island 4.

**Inaugural-Dissertation**
**zur Erlangung des Doktorgrades**
**der Zahnheilkunde**

**der Medizinischen Fakultät**
**der Eberhard Karls Universität**
**zu Tübingen**

**vorgelegt von**

**Kohler, Alexander Antonius**

**2023**

| | |
|---|---|
| Dekan: | Professor Dr. B. Pichler |
| 1. Berichterstatter: | Professor S. Wagner, PhD |
| 2. Berichterstatter: | Privatdozent Dr. E. Bohn |
| Tag der Disputation: | 09.12.2022 |

## Table of contents

## Abbreviations

| | |
|---|---|
| aa | amino acids |
| ABC-transporter | ATP-binding cassette transporter |
| BIg | bacterial Immunoglobulin |
| BN | Blue Native |
| bp | base pair |
| C26 | Compound 26 |
| CFU | colony forming unit |
| DMSO | dimethyl sulfoxide |
| *E. coli* | *Escherichia coli* |
| EDTA | ethylenediaminetetraacetic acid |
| Gluc | *Gaussia princeps* luciferase |
| kb | kilobase |
| kDa | kilodalton |
| LB | Luria broth |
| LMNG | lauryl maltose neopentyl glycol |
| MDCK cells | Madin-Darby canine kidney cells |
| MFP | membrane fusion protein |
| MOI | multiplicity of infection |
| Nluc | NanoLuc luciferase |
| $OD_{600}$ | optical density at a wavelength of 600 nm |
| ODU | optical density units (per milliliter) |
| OMP | outer membrane protein |
| PAGE | polyacrylamide gel electrophoresis |
| RLU | relative light units |
| rpm | revolutions per minute |
| RT | room temperature |
| RTX | repeats in toxin |
| *S.* Typhimurium | *Salmonella* Typhimurium |
| SDS | sodium dodecyl sulfate |
| SPI-1 | *Salmonella* pathogenicity island 1 |
| SPI-4 | Salmonella pathogenicity island 4 |
| T1SS | type I secretion system |
| T3SS-1 | type III secretion system encoded on SPI-1 |
| *Taq* | *Termus aquaticus* |
| WT | wild type |

## List of figures and tables

# 1 Introduction

Antimicrobial resistance is one of the biggest public health threats humanity is facing (WHO 2021). Each year 700,000 lives are lost due to infectious diseases caused by antimicrobial resistant pathogens, which are hard to treat with the currently available antibiotics (CDC 2019; WHO 2019, 2020, 2021). As this development proceeds, 10 million patients could die from drug-resistant diseases each year by 2050 (WHO 2019).

A novel approach in fighting against bacterial infections is the development of anti-virulence agents that target specific disease-relevant mechanisms (called virulence factors), instead of generating a life-or-death pressure (Cegelski et al. 2008; Wang et al. 2020). As anti-virulence agents do not kill or interfere with the bacterial growth, it is suggested that selective pressure and development of resistance are reduced (Cegelski et al. 2008; Wang et al. 2020). Furthermore, it is believed that these new drugs would not affect the homeostasis of the intestinal microbiota in the gut (Cegelski et al. 2008).

The lab of Samuel Wagner has been developing a small molecule called Compound 26 (C26) as an anti-virulence agent against infections with *Salmonella* Typhimurium. C26 targets the main transcriptional regulator of *Salmonella* pathogenicity HilD (Abdelhakim Boudrioua, personal communication 2021).
The following work aims to quantify the effect of C26 on *Salmonella* pathogenicity island 4 (SPI-4). First, *Salmonella* pathogenicity and the regulatory network will be described in order to understand the target of the anti-virulence agent C26.

## 1.1 *Salmonella*: Classification, disease and treatment

*Salmonella* is a facultative intracellular Gram-negative bacterium from the family of Enterobacteriaceae. It has a rod-like shape, is sized between 2 - 3 µm and characterised by flagella-driven motility (Chlebicz and Śliżewska 2018).

The nomenclature of *Salmonella* is complex and reviewed in Ryan et al. 2017. *Salmonella* is classified into two species: *Salmonella enterica* and *Salmonella bongori*. *Salmonella enterica* comprises six subspecies. The Kaufmann-White classification distinguishes between almost 2,600 serovars depending on the O- and H-antigens. *Salmonella enterica* subspecies *enterica* comprises most serovars (1,586 serovars) (Ryan et al. 2017).

*Salmonella enterica* subspecies *enterica* causes 99 % of *Salmonella* infections in humans and animals (Chlebicz and Śliżewska 2018). Depending on the serovar, *Salmonella enterica* infection can lead to typhoid fever or salmonellosis (including gastroenteritis) (RKI 2016; Ryan et al. 2017).

The most life-threatening infections, typhoid and paratyphoid fevers, are caused by *Salmonella enterica* subsp. *enterica* serovar Typhi and Paratyphi (RKI 2008; Ryan et al. 2017). Although outbreaks in Europe are rare and more common in developing countries, there are 21 million cases and 200,000-related deaths due to typhoid fever each year worldwide (RKI 2008; Ryan et al. 2017; Chlebicz and Śliżewska 2018).

The remaining serovars from *Salmonella enterica* subspecies *enterica* cause salmonellosis, which is one of the most common food-borne zoonoses (Chlebicz and Śliżewska 2018). This large group is also referred to as Non-typhoidal *Salmonella* (NTS) (Ryan et al. 2017). It is estimated that each year NTS causes 93.8 million cases of gastroenteritis and 155,000 people die from the consequences worldwide (Majowicz et al. 2010).
NTS colonises predominantly the intestine of food-producing animals and is transmitted by contaminated water or animal products like meat from poultry, pigs and cattle or raw eggs (WHO 2018). Transmission can also occur through contaminated raw vegetables or fruit (WHO 2018).

The infectious dose in adults is about $10^4$ - $10^6$ CFUs (colony forming units) (RKI 2016). NTS usually causes a self-limited gastroenteritis with diarrhea, fever,

abdominal pain and occasionally nausea, headache or vomiting. These symptoms generally appear 12 - 36 h after infection (RKI 2016; WHO 2018; CDC 2021).

In predisposed risk groups like immunocompromised, children or elderly patients, the infectious dose is under $10^2$ CFUs. In these cases *Salmonella* can also cause extra-intestinal infections or trigger sepsis (RKI 2016; WHO 2018). *S*. Enteritidis and *S*. Typhimurium are the two most common serovars responsible for salmonellosis in humans (WHO 2018).

Rather than with antibiotics, gastroenteritis without signs of systemic infection is routinely treated with substitution of liquid and electrolytes. According to the german “S2k-Leitlinie” from 2015 for gastrointestinal infections (AWMF-Register-Nr. 021/024), antibiotic treatment should take place in case of systemic infection, bacteremia, immunocompromised patients and hemodialysis patients. The antibiotics of choice are ciprofloxacin or ceftriaxone (S2k-Leitlinie 2015). Due to the increasing number and wide spread of antibiotic resistant *Salmonella* serovars *(Nair et al. 2018; Jajere 2019)*, antibiotic resistance should be tested in advance. The Centers for Disease Control and Prevention (CDC) reports an estimated number of 41,000 and 89,200 cases of *Salmonella* infections in the U.S. per year which are resistant to ceftriaxone or ciprofloxacin non-susceptible, respectively (CDC 2019).

*S*. Typhimurium pathogenicity is briefly summarised, in order to understand how C26 inhibits virulence factors and disarm the bacterium.

*S*. Typhimurium possesses a variety of virulence factors. The majority is encoded on specific, highly conserved areas of the chromosome, so called *Salmonella* pathogenicity islands (SPIs) (Fàbrega and Vila 2013; Jajere 2019). *S*. Typhimurium possesses five SPIs (SPI-1 to SPI-5) (reviewed in Fàbrega and Vila 2013).

## 1.2 *Salmonella* pathogenicity island 1 (SPI-1)

SPI-1 encodes a type 3 secretion system (T3SS) (reviewed in Wagner et al. 2018) that enables *S*. Typhimurium to inject a cocktail of effector proteins directly

into the host cell cytoplasm. These effector proteins induce actin rearrangement and the engulfment of *Salmonella* into the eukaryotic host cell (Fàbrega and Vila 2013).

T3SSs are widespread among Gram-negative pathogenic bacteria (Deng et al. 2017; Wagner et al. 2018). This secretion system consists of almost 20 proteins, forming the export apparatus in the inner membrane, cytoplasmic components, a base that spans the inner and outer membrane and the 20 - 150 nm long needle filament with the translocation pore in the host cell membrane (Wagner et al. 2018). Beside the T3SS, SPI-1 also encodes effector proteins, chaperons and transcriptional regulators, among them the main transcriptional regulator for *Salmonella* pathogenicity HilD (Lou et al. 2019). HilD controls the expression of SPI-1 virulence genes and genes located outside of SPI-1 (Smith et al. 2016).

After internalisation in the host cell, a second T3SS (T3SS-2), which is encoded by genes on SPI-2, is responsible for intracellular survival and replication inside the *Salmonella*-containing vacuole (SCV) (Hensel 2000).

Taken together, due to their important role during intestinal infection and their high degree of conservation among Gram-negative bacteria, T3SSs are a promising and powerful target for novel anti-virulence agents (Hotinger et al. 2021; Hussain et al. 2021). T3SS-1 inhibitors include natural and artificial compounds that can target T3SS-1 structural components or even regulatory genes (Hussain et al. 2021).

## 1.3 *Salmonella* pathogenicity island 4 (SPI-4)

### 1.3.1 Genetic organisation of SPI-4

The 27 kb long SPI-4 was first described in 1998 using a genome-wide approach and predicted to include 18 open reading frames (ORFs) (Wong et al. 1998). The complete genome sequence of *S*. Typhimurium LT2 revealed that SPI-4 contains only six ORFs, annotated as STM4257-STM4262 (signature tagged mutagenesis) (McClelland et al. 2001). Investigation of SPI-4 pathogenicity *in*

*vivo* revealed that SPI-4 contributes to intestinal colonisation of calf after oral infection (Morgan et al. 2004; Morgan et al. 2007). Thus, genes on SPI-4 were annotated as *siiA-F*, for *Salmonella* intestinal infection (Figure 1a) (Morgan et al. 2004).
The six genes encoded on SPI-4 most likely form one 24 kb large transcriptional unit (Gerlach et al. 2007a; Main-Hester et al. 2008). The transcriptional start site is located 470 bp upstream of *siiA* (Main-Hester et al. 2008).

Sequence analysis of *S*. Typhimurium NCTC 12023 predicted that the genes *siiB-D* overlap and suggested the presence of an intergenic region of 107 bp between *siiA-B*, one of 16 bp between *siiD-E* and a third one of 39 bp between *siiE-F* (Gerlach et al. 2007a).
A previous genome analysis of *S*. Typhimurium SL1344 revealed that in this strain the *siiA-D* genes overlap and the intergenic regions between *siiD-E* and *siiE-F* comprise 20 bp and 40 bp, respectively (Main-Hester et al. 2008).
However, in the SL1344 strain used in this study (Table 4), the intergenic regions between *siiD-E* and *siiE-F* comprise 19 bp and 39 bp, respectively (Figure 1a) (Abdelhakim Boudrioua, personal communication 2021).

There is an operon polarity suppressor (*ops*) element upstream of *siiA (Morgan et al. 2004)* that enhances transcriptional elongation together with the antiterminator protein RfaH (Main-Hester et al. 2008).
This is especially important for distal genes like *siiE* (Kiss et al. 2007; Main-Hester et al. 2008). Expression of *siiF* is less influenced by RfaH/*ops* mutations (Gerlach et al. 2007a; Main-Hester et al. 2008). This could be due to a second independent promoter upstream of *siiF* (Main-Hester et al. 2008).
Based on sequence analysis, SiiC, SiiD and SiiF are predicted to be components of the type I secretion system (T1SS) encoded on SPI-4 (Morgan et al. 2004), which mediates secretion of the giant non-fimbrial adhesin SiiE into culture supernatant (Gerlach et al. 2007b; Kiss et al. 2007; Morgan et al. 2007; Main-Hester et al. 2008). The general structure of a T1SS is characterised in the following section (1.3.2).

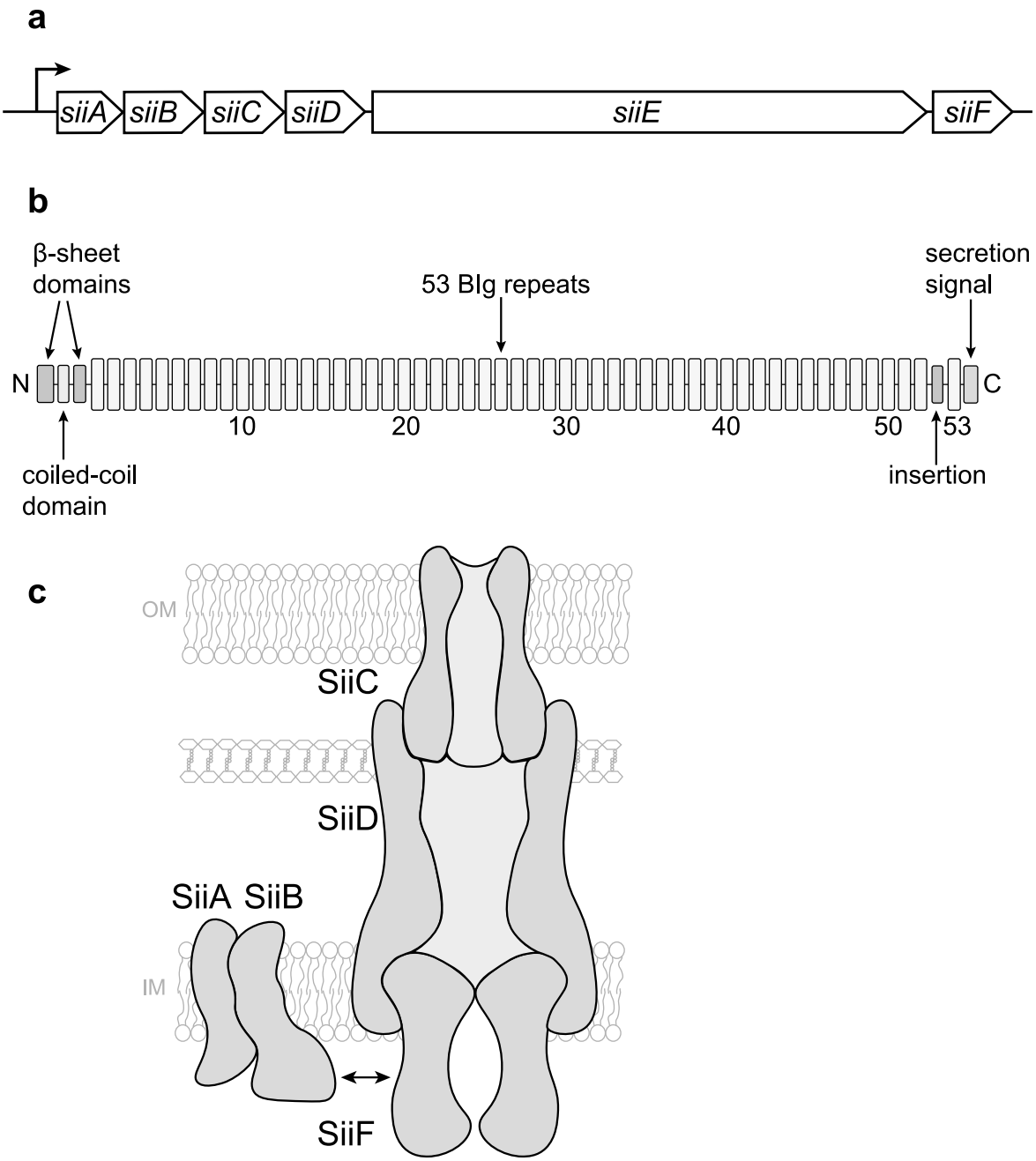


**Figure 1: SPI-4 genetic organisation, SiiE structure and scheme of the T1SS.**
(a) Transcriptional organisation of SPI-4. Intergenic regions of 19 bp and 39 bp between *siiD-siiE* and *siiE-siiF*, respectively. The promotor (bent arrow) is located upstream of *siiA*. Scheme is not to scale. Scheme was adapted from Gerlach et al. 2007a; Main-Hester et al. 2008.
(b) Scheme of SiiE structure with 53 bacterial Immunoglobulin (BIg) repeats. The amino (N)-terminus with two β-sheet and one coiled-coil domain is shown. The carboxy (C)-terminus contains the secretion signal. The insertion of 51 aa with unknown function between BIg52 and BIg53 is marked. Scheme of SiiE is not to scale. Figure was adapted from Gerlach et al. 2007b; Wagner et al. 2011.
(c) Scheme of T1SS structure. SiiC, SiiD and SiiF are components of the T1SS encoded on SPI-4 (Morgan et al. 2004; Gerlach et al. 2007b). SiiA and SiiB form a proton-conducting channel in the inner membrane and the double-headed arrow denotes protein interaction between SiiB and SiiF (Wille et al. 2014; Kirchweger et al. 2019). IM and OM, bacterial inner and outer membranes, respectively. T1SS structure was adapted from Costa et al. 2015.

### 1.3.2 Type I secretion system (T1SS)

Type I secretion systems (T1SSs) are widespread among Gram-negative bacteria which use it to secrete substrates from the bacterial cytoplasm into the extracellular space (Lenders 2015; Kanonenberg et al. 2018; Spitz et al. 2019). Among the T1SS substrates are virulence factors like adhesins and pore-forming toxins (Costa et al. 2015; Kanonenberg et al. 2018; Spitz et al. 2019), but also factors for nutrient acquisition like iron scavenger proteins (Costa et al. 2015).
T1SS substrates are transported across the two bacterial membranes into the extracellular space as unfolded proteins in a process that occurs without a periplasmic intermediate (Costa et al. 2015; Lenders 2015; Spitz et al. 2019). T1SS substrates contain a secretion signal in the last 50 to 100 aa of their C-terminus and that is sufficient for secretion (Kanonenberg et al. 2018).
Compared to other secretion systems like the sophisticated T3SS, which can even inject effector proteins directly into the host cell cytoplasm, the tunnel channel structure of T1SS is relatively simple and requires only three membrane proteins (Figure 1c) (Costa et al. 2015; Kanonenberg et al. 2018). In general, T1SSs consist of two inner membrane proteins, an ATP-binding cassette transporter (ABC-transporter) and a membrane fusion protein (MFP) (Lenders 2015; Kanonenberg et al. 2018). The pore forming outer membrane protein (OMP) is the third component of the T1SS (Lenders 2015; Kanonenberg et al. 2018). The T1SS that mediates secretion of the pore-forming hemolysin A (HlyA) in *E. coli* is the best studied T1SS (Lenders 2015; Kanonenberg et al. 2018; Spitz et al. 2019; Beer 2020), although the complex structure remains to be determined experimentally (Jo et al. 2019). However, the general function of the T1SS is shown exemplarily for the HlyA secretion machinery.

Estimations of the HlyA T1SS stoichiometry are based on cross-linking experiments revealing that the dimeric ABC-transporter HlyB and the trimeric MFP HlyD form a stable complex in the inner membrane (Spitz et al. 2019). This could also be the case for the T1SS encoded on SPI-4 as previously suggested (Wille et al. 2014). However, it is still under debate whether the MFP HlyD is a hexamer or trimer (Kanonenberg et al. 2018; Jo et al. 2019; Spitz et al. 2019;

Beer 2020). The OMP TolC is a trimeric protein (Jo et al. 2019) and only recruited to the HlyB-HlyD complex in presence of the substrate HlyA (Spitz et al. 2019). The latter is secreted as unfolded protein with its C terminus first, a process that is energised by ATP hydrolysis. At the cell surface, $Ca^{2+}$ ions bind to repeats in toxins (RTX) and induce folding of HlyA (Kanonenberg et al. 2018; Spitz et al. 2019). The current knowledge of structure, assembly and function of T1SS was recently reviewed in Kanonenberg et al. 2018; Spitz et al. 2019; Alav et al. 2021.

In the context of the SPI-4 encoded T1SS, SiiF is predicted to be the inner membrane ABC-transporter, SiiD the MFP and SiiC the OMP (Figure 1c) (Morgan et al. 2004; Gerlach et al. 2007b; Main-Hester et al. 2008). Mutations in *siiC*, *siiD* or *siiF*, respectively abolish SiiE secretion, but they do not compromise SiiE expression (Gerlach et al. 2007b; Kiss et al. 2007; Morgan et al. 2007; Main-Hester et al. 2008). SiiA and SiiB were described as novel components of the SPI-4 encoded T1SS (Figure 1c), which form a proton-conducting channel within the inner membrane and control SiiE surface fixation and release (Wagner 2011; Wille et al. 2014; Kirchweger et al. 2019).
Recently, the first step towards deeper functional and structural understanding was made with the successful report of protein production and purification of SiiF, SiiD and SiiE variants (Klingl et al. 2020).
*Salmonella enterica* possesses a variety of different adhesins, which are summarised before the giant non-fimbrial adhesin SiiE is described.

### 1.3.3 *Salmonella* adhesiome

The adhesiome of *Salmonella enterica* comprises up to 20 adhesins which are categorised in fimbrial and non-fimbrial adhesins (Gerlach and Hensel 2007; Hansmeier et al. 2017). Fimbrial and non-fimbrial adhesins differ in terms of structure and assembly mechanism (Gerlach and Hensel 2007; Barlag and Hensel 2015). The variety of the *Salmonella* adhesiome could be the consequence of adaption to different hosts (Gerlach and Hensel 2007; Hansmeier et al. 2017).

Fimbrial adhesins are polymers of several subunits, integrated in the outer bacterial membrane and bind to receptors on the host cell surface (Gerlach and Hensel 2007; Rehman et al. 2019). There are 13 fimbrial adhesins in *S*. Typhimurium including 12 fimbriae assembled by the chaperone-usher (CU) pathway (Wagner 2011; Hansmeier et al. 2017). Thin aggregative fimbriae (Tafi), which are also known as curli in *E*. *coli*, are assembled by extracellular nucleation precipitation (Gerlach and Hensel 2007; Wagner 2011; Hansmeier et al. 2017; Rehman et al. 2019).

Non-fimbrial adhesins are secreted by an autotransporter or T1SS (Barlag and Hensel 2015). The trimeric autotransported adhesins (TAA) MisL (SPI-3), ShdA (CS54 island) and SadA are secreted through an autotransporter, which is also named type V secretion system (T5SS) (Barlag and Hensel 2015; Hansmeier et al. 2017).
The second group of non-fimbrial adhesins includes the two adhesins BapA and SiiE, which are secreted through a T1SS (Gerlach and Hensel 2007; Barlag and Hensel 2015; Hansmeier et al. 2017).

#### 1.3.3.1 Giant non-fimbrial adhesin SiiE

The giant non-fimbrial adhesin SiiE mediates adhesion of *S*. Typhimurium to polarised monolayers of MDCK, CaCo-2 and T-84 cells (Gerlach et al. 2007b). SiiE-mediated adhesion is a prerequisite for invasion of polarised epithelial cells (MDCK, CaCo-2) from the apical side, which is rich in microvilli (Gerlach et al. 2008). On the contrary, SPI-4 function is not required for invasion of non-polarised HeLa cells or the invasion of polarised cells from the baso-lateral side (Gerlach et al. 2008).

SiiE consists of 53 bacterial Immunoglobulin (BIg) domains (Figure 1b) and is the largest protein in *Salmonella*, with a molecular weight of 595 kDa (Gerlach et al. 2007b; Main-Hester et al. 2008). Its length of approximately 175 ± 5 nm may be necessary to protrude extracellularly through the LPS layer to mediate adhesion to the target host cell membrane (Gerlach et al. 2008; Wagner et al. 2011). Li et

al. proposed a model in which SiiE facilitates contact and positions the 80 nm long T3SS-1 injectisome to the apical host cell membrane, where up to 200 nm long transmembrane mucins like MUC1 impede easy access (Li et al. 2019).

SiiE is secreted into the supernatant (Gerlach et al. 2007b; Kiss et al. 2007; Morgan et al. 2007; Main-Hester et al. 2008) and is temporarily expressed on the bacterial surface (Wagner et al. 2011). The phase of highest SiiE surface retention correlates with the phase of highest invasion capacity of polarised epithelial cells (Wagner et al. 2011).
Wagner et al. investigated SiiE structure and function and could show that the β-sheet#1, the coiled-coil and the β-sheet#2 domain located at the N-terminus of SiiE (Figure 1b) are essential for controlled SiiE surface retention and release (Wagner et al. 2011). It was proposed that SiiE is temporarily fixed in the T1SS channel, then binds to the eucaryotic cell surface (Wagner et al. 2011). Interestingly, impaired adhesion and invasion capacity of *siiE* or *siiF* deficient mutants cannot be reconstituted by the addition of SiiE containing supernatant (Gerlach et al. 2007b; Wagner et al. 2011).
Although the inner membrane proteins SiiA and SiiB are not required for SiiE secretion into supernatant (Gerlach et al. 2007b; Kiss et al. 2007; Main-Hester et al. 2008), adhesion and invasion capacity of *Salmonella* into polarised monolayers of MDCK cells is strongly attenuated in *siiA* or *siiB* mutants (Wille et al. 2014).
In the current working model SiiA and SiiB form a proton channel in the inner membrane that uses the proton-motive force (PMF) for regulation of SiiE surface retention and release through an unknown mechanism (Figure 1c) (Wagner 2011; Wagner et al. 2011; Wille et al. 2014; Kirchweger et al. 2019).

However, temporary retention of T1SS substrates is also described for LapA, the large adhesin of *Pseudomonas fluorescens*, which is anchored with its N-terminal “retention module” to the OMP LapE (Barlag and Hensel 2015; Spitz et al. 2019). LapA can be released from the T1SS through controlled cleavage by the protease LapG, depending on the environmental conditions either suitable for biofilm

formation or not (Barlag and Hensel 2015; Spitz et al. 2019; Alav et al. 2021). The ice-binding adhesin (IBA) of *Marinomonas primoryensis* is also anchored to the T1SS with a putative N-terminal plug, similar to LapA (Spitz et al. 2019).

The secretion signal of SiiE is localised in the last 125 aa at the C-terminus, comprising the BIg53 and the last C-terminal domain (Figure 1b) (Wagner 2011). The insertion of 51 aa between BIg52 and BIg53 is required neither for SiiE secretion nor fixation or adhesion (Wagner et al. 2011). Its role is yet to be elucidated.
C-terminal BIg domains mediate binding to N-acetylglucosamine (GlcNAc) and/or *α* 2,3-linked sialic acid containing glycostructures at the target host cell membrane in a zipper-like manner (Wagner et al. 2014; Li et al. 2019). It was recently shown that the glycosylated transmembrane mucin MUC1 on the apical surface of enterocytes is bound by SiiE and required for SiiE mediated host cell invasion (Li et al. 2019).

Investigation of SPI-4 pathogenicity in animal models revealed that SPI-4 contributes to intestinal colonisation of calf after oral infection (Morgan et al. 2004; Morgan et al. 2007). On the contrary, SPI-4 is not required for intestinal colonisation in chickens (Morgan et al. 2004) or pigs (Morgan et al. 2007).
Different observations were made regarding SPI-4 pathogenicity in mice models. There are reports that SPI-4 contributes to systemic colonisation (liver, spleen) in mice after oral infection (Morgan et al. 2004; Kiss et al. 2007). But it was also reported by Gerlach et al. that SPI-4 does not contribute to systemic virulence in mice after oral infection (Gerlach et al. 2007b). One explanation for the discrepancy could be that different infectious doses were used (Gerlach et al. 2007b).

## 1.4 SPI-1 regulatory network

The coordinated and controlled expression of virulence factors at the right time and place, under the best environmental conditions for invasion or intracellular survival, is crucial for efficient host cell colonisation and *Salmonella* pathogenesis

(reviewed in Fàbrega and Vila 2013). Most transcriptional regulators of the SPI-1 regulatory network are encoded within SPI-1 and control the expression of genes within and outside SPI-1 (Fàbrega and Vila 2013; Lou et al. 2019). In the intestine, expression of the SPI-1 is regulated by specific environmental factors, such as oxygen level, osmolarity, pH and temperature (Ibarra et al. 2010; Deng et al. 2017), but also bile and short chain fatty acids (Lou et al. 2019).

Important for this work and the anti-virulence activity of C26 is the coregulation of SPI-1 and SPI-4 gene expression by the same transcriptional activator hyper invasion locus A (HilA) and regulatory system (Ahmer et al. 1999; Gerlach et al. 2007a; Main-Hester et al. 2008).

A simplified model of the SPI-1 regulatory network is shown in Figure 2 (reviewed in Fàbrega and Vila 2013; Lou et al. 2019).

The transcriptional activator HilA is central to the regulatory network (Ellermeier and Slauch 2007; Lou et al. 2019). Deletion of *hilA* leads to the same loss of invasion capacity in mice as the deletion of the whole SPI-1 locus (Ellermeier et al. 2005).

While initial studies reported the existence of a negative feedback regulation for HilA (De Keersmaecker et al. 2005), new observations point to the possibility that HilA might not be negatively autoregulated (Kalafatis and Slauch 2021).

Ellermeier et al. were the first to describe the feedforward regulatory loop formed by the DNA-binding proteins HilD, HilC and RtsA, which controls and regulates *hilA* expression (Figure 2) (Ellermeier et al. 2005). HilD, HilC and RtsA are homologous proteins belonging to the AraC-family and can independently activate *hilA* but also *hilD, hilC* and *rtsA* gene expression (Ellermeier et al. 2005; Narm et al. 2020). However, HilD is at the top of the regulatory hierarchy and the most powerful transcriptional activator of *hilA* (Ellermeier and Slauch 2007). In absence of HilD there is no expression of *hilA* and SPI-1 gene expression is therefore shut down (Ellermeier et al. 2005; Saini et al. 2010). HilC and RtsA act as transcriptional amplifiers for HilD and the feedforward regulatory loop self-reinforces the signal to sufficiently activate *hilA* and SPI-1 gene expression (Ellermeier and Slauch 2007; Saini et al. 2010).

Most environmental signals feed into the regulatory circuit at the level of HilD (Figure 2) (Ellermeier and Slauch 2007), largely controlling HilD at the translational level (Ellermeier et al. 2005; Martínez et al. 2011; Golubeva et al. 2012). HilE is an important negative regulator that binds HilD and thereby decreases its DNA binding capacity (Grenz et al. 2018; Paredes-Amaya et al. 2018).

*Salmonella* recognises environmental changes via two-component systems that comprise a membrane bound sensor and a response regulator (Fàbrega and Vila 2013). The PhoQP, PhoRB and BarA/SirA two component systems are shown in Figure 2 and described briefly.

The PhoQP two component system negatively regulates *hilA* gene transcription dependent on environmental conditions similar to the intracellular milieu (Palmer et al. 2019). This includes low levels of cations, low pH and antimicrobial peptides (García Véscovi et al. 1996; Groisman 2001). Thus, PhoQP is important for the controlled shut down of SPI-1 T3SS gene expression, which is not required for intracellular survival (Palmer et al. 2019). Palmer et al. have reported that PhoP inhibits direct activation of the *hilA* promoter through HilD, HilC and RtsA, and presumably reduces *hilD* and *rtsA* transcription (not shown in Figure 2), although the latter mechanism remains to be elucidated (Palmer et al. 2019). PhoP further induces transcription of the sRNA PinT, which represses *hilA* and *rtsA* translation (Kim et al. 2019).

The PhoRB two component system senses low extracellular phosphate conditions and negatively regulates *hilA* expression (Baxter and Jones 2015). PhoRB induces *fimZ* expression, which increases *hilE* expression and thus inhibits expression of *hilA* (Figure 2) (Baxter and Jones 2015).

The two component regulatory system BarA/SirA positively regulates *hilD* expression and is presumably directly activated by gut environmental cues like short-chain fatty acids (Ellermeier et al. 2005; Lou et al. 2019). SirA increases expression of the sRNAs CsrB and CsrC, which bind and inhibit CsrA, an RNA

binding protein that binds HilD mRNA and inhibits its translation (Fàbrega and Vila 2013). Thus, SirA increases HilD translation (Fàbrega and Vila 2013). Pérez-Morales et al. could show that SirA also increases HilE translation. This means that BarA/SirA simultaneously exerts both, a direct positive effect on HilD and an indirect negative effect on HilD by increasing HilE translation (Figure 2) (Pérez-Morales et al. 2021). This was described as an incoherent type-1 feedforward loop which is crucial to reduce the growth retardation associated with the expression of HilD induced pathogenicity genes (Pérez-Morales et al. 2021).

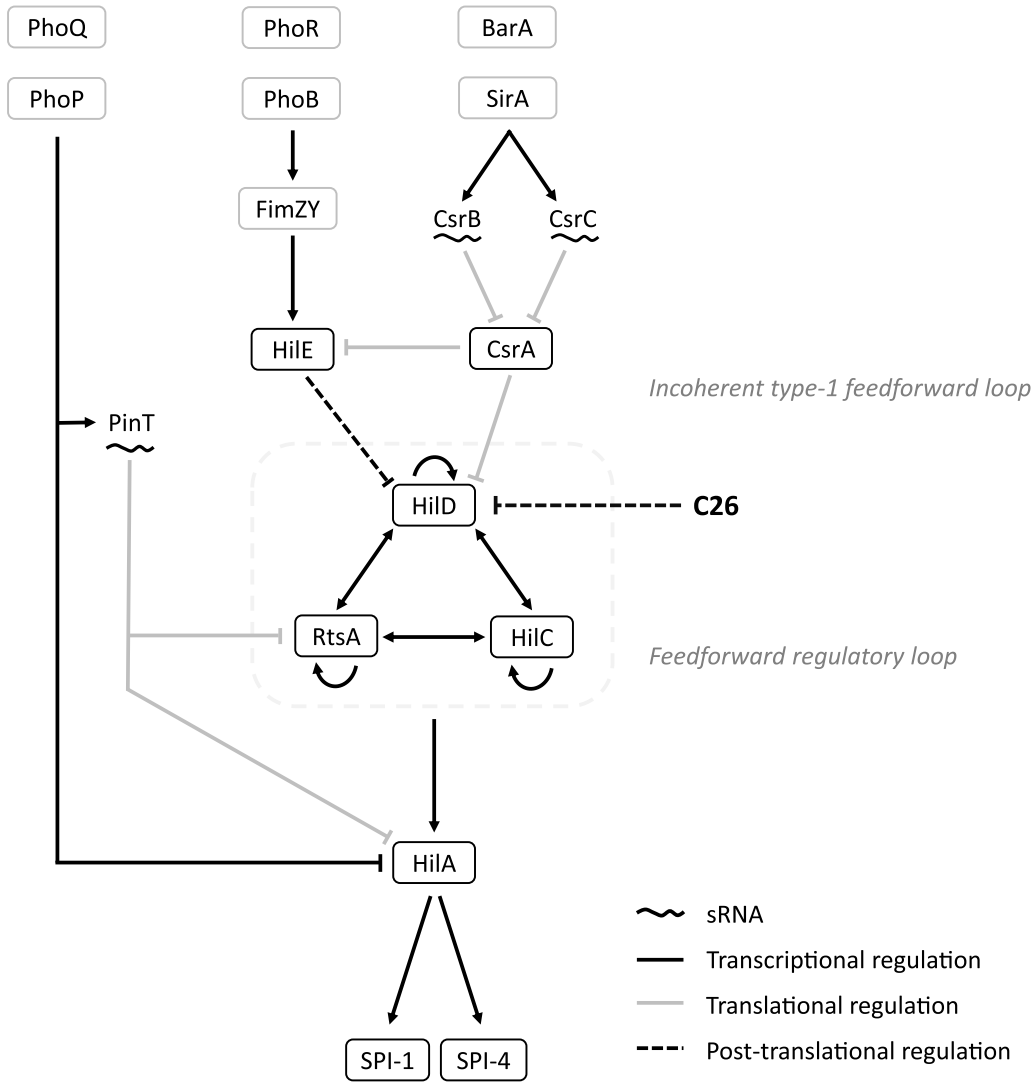


**Figure 2: Simplified model of SPI-1 regulatory network.**
C26 inhibits the HilD activity (Samuel Wagner, Abdelhakim Boudrioua, personal communication 2021). Black lines indicate transcriptional regulation, grey lines represent translational regulation and dashed lines point to regulation at the protein level. Positive effects are shown by an arrowhead, negative effects by a flathead. Scheme adapted from Ellermeier and Slauch 2007; Main-Hester et al. 2008; Fàbrega and Vila 2013; Kim et al. 2019; Palmer et al. 2019; Pérez-Morales et al. 2021.

### 1.4.1 Regulation of SPI-4

The model of the SPI-1 regulatory network can be transferred to SPI-4 as both SPIs are regulated by HilA and SirA (Figure 2) (Ahmer et al. 1999; Ellermeier and Slauch 2003; Gerlach et al. 2007a; Thijs et al. 2007; Main-Hester et al. 2008). The tight coregulation can be seen as a consequence of the coordinated activity of SPI-1 and SPI-4 that is required for invasion of polarised epithelial cells (Gerlach et al. 2007a; Gerlach et al. 2008).
Saini and Rao described the transcriptional regulator SprB encoded on SPI-1 as an activator of the *siiA* promoter and the link between SPI-1 and SPI-4 expression (Saini and Rao 2010). However, Smith et al. observed no binding to and regulation of SPI-4 genes through SprB (Smith et al. 2016). Main-Hester et al. reported no reduction of *siiE* expression in a *sprB* mutant (Main-Hester et al. 2008).

The central regulator HilA binds a region (STM4256) upstream of *siiA* (Thijs et al. 2007). The HilA-binding site is likely to be located downstream of the *sii* promoter (Main-Hester et al. 2008). There are inconsistent reports about an additional HilA binding site inside the *siiE* gene (STM4261) (De Keersmaecker et al. 2005; Thijs et al. 2007).
However, Main-Hester et al. proposed that HilA activates SPI-4 expression most likely by replacing histone-like nucleoid structuring proteins (H-NS) (Main-Hester et al. 2008). H-NS are nucleoid-associated proteins that bind to AT-rich DNA sequences of horizontally acquired genes and thereby inhibit uncontrolled expression of foreign DNA (Lucchini et al. 2006; Navarre et al. 2007). Main-Hester et al. observed that *siiE* is expressed independently from HilA in an *h-ns* mutant and that the predicted HilA-binding site overlaps with a region bound by H-NS (Main-Hester et al. 2008).

Most strikingly, however, although SPI-4 expression is most likely activated through HilA, *siiA* expression was reduced only 6.3-fold in a *hilA* mutant, whereas deletion of SirA led to a 97-fold reduction of *siiA* expression (Gerlach et al. 2007a). HilA alone cannot activate SPI-4 expression, suggesting that another

regulator is involved in SPI-4 regulation (Gerlach et al. 2007a; Main-Hester et al. 2008). Experiments performed in *E*. *coli* revealed that HilD and its homologues HilC and RtsA can bind and directly activate transcription of *siiA* (Petrone et al. 2014). The binding sites of HilD, HilC and RtsA on *siiA* overlap with regions that are likely bound by H-NS (Smith et al. 2016). However, further work must elucidate the regulatory network of SPI-4.

## 1.5 Objectives

Our lab has shown that C26 targets the main transcriptional regulator HilD and strongly reduces T3SS-1 dependent secretion of effector proteins with an IC50 of 29 µM (Abdelhakim Boudrioua, personal communication 2021). The cytotoxicity to HeLa cells is very low and preliminary experiments revealed that C26 reduces *Salmonella* invasion of HeLa cells (Samuel Wagner, personal communication 2021).

The aim of this work was to investigate the effect of the HilD inhibitor C26 on *Salmonella* pathogenicity island 4 (SPI-4).

First, expression of the ABC-transporter protein SiiF and the assembly of the T1SS (SiiCDF) in presence of different concentrations of C26 were assessed.
Second, a NanoLuc luciferase-based assay was established which allows quantification of SiiE secretion in presence of C26.
Lastly, polarised MDCK cell monolayers should have been established to assess the effect of C26 on SPI-4 mediated adhesion to polarised cells and T3SS-1 dependent host cell invasion.
The effect of C26 and the role of SPI-4 mediated adhesion for T3SS-1 effector protein injection into HeLa cells was also investigated.

Together with previous results that proved the inhibition of T3SS-1 (Abdelhakim Boudrioua, personal communication 2021), this work was aimed to strengthening and confirming the role of C26 as a promising new candidate for antimicrobial therapy.

# 2 Material and Methods

## 2.1 Media, buffers and antibodies

### 2.1.1 Media and culture conditions

For the cloning procedure *Escherichia coli* (*E*. *coli*) and *S*. Typhimurium strains were grown overnight in 3 ml liquid LB medium in glass tubes or in 10 ml LB in 50 ml Falcon tubes at 37°C, 180 rpm. 100 µg/ml diaminopimelic acid (DAP) was added to the medium for growth of *E*. *coli* β2163.

If not mentioned otherwise, for induction of SPI-1 and SPI-4 gene expression *in vitro*, *S*. Typhimurium strains (Table 4) were grown o/n in 3 ml LB 0.3 M NaCl medium in glass tubes with low aeration (Bajaj et al. 1996). The next day, the $OD_{600}$ was measured and strains were subcultured to a $OD_{600}$ of 0.05 in 3 ml (for SiiE secretion assay, injection and invasion assay) or 10 ml (for crude membranes) LB 0.3 M NaCl medium (Table 2) in glass tubes or 50 ml Falcon tubes, respectively.
Subcultures were grown for 3.5 or 5 h, as indicated. This ensures that strains were in the late exponential growth phase with maximal SPI-1 and SPI-4 gene expression.
As indicated, different concentrations of the compound C26 in 1 % DMSO or only 1 % DMSO as a control were added to the subcultures. C26 was synthesised by Mark Brönstrup Lab at the Helmholtz centre for infection research in Braunschweig, Germany (Abdelhakim Boudrioua, personal communication 2021).
For all conditions, the respective antibiotics were added to LB or LB 0.3 M NaCl in the following concentrations (Table 1).

Table 1: Used antibiotics with concentrations

| Antibiotics | Final concentration |
|---|---|
| Streptomycin (Strep) | 50 µg/ml |
| Tetracycline (Tet) | 12.5 µg/ml |
| Ampicillin (Amp) | 100 µg/ml |

Table 2: Media, buffers and solutions used in this study

| Name | Composition |
|---|---|
| **Media for cultivation of bacteria** | |
| LB agarose plates | 10 g LB Lennox and 7.5 g agar were dissolved in 500 ml $H_2O$ and sterilised in the autoclave. Corresponding antibiotics were added to the 50°C warm agar prior pouring the petri dishes. |
| LB/Tet/DAP agarose plates | 20 g LB Lennox, 15 g agar were dissolved in 1 l $H_2O$ and sterilised in the autoclave. Then, 480 µl of 12.5 mg/ml Tetracycline and 20 ml of 5 mg/ml DAP was added under sterile conditions to the 50°C warm agar prior pouring the petri dishes. |
| LB/Strep/sucrose agarose plates | 5 g tryptone, 2.5 g yeast extract and 7.5 g agar were dissolved in 400 ml $H_2O$ and sterilised in the autoclave. Prior pouring the petri dishes, 100 ml sterile filtered (0.22 µm) 50 % (w/v) sucrose and streptomycin were added to the 50°C warm agar. |
| LB medium | 5 g NaCl, 10 g tryptone and 5 g yeast extract were dissolved in 1 l $H_2O$ and sterilised in the autoclave. |
| LB 0.3 M NaCl medium | 12.5 g NaCl, 10 g tryptone and 5 g yeast extract were dissolved in 1 l $H_2O$ and sterilised in the autoclave. |
| SOB medium (super optimal broth) | 40 g bacto-tryptone, 10 g yeast extract, 1 g NaCl and 0.373 g KCL were dissolved in 2 l $H_2O$ and sterilised in the autoclave. Sterile filtered (0.22 µm) 1 M $MgCl_2$ and 1 M $MgSO_4$ solutions were added to a final concentration of 10 mM. |
| SOC medium (super optimal broth with catabolite repression) | 20 ml sterile filtered (0.22 µm) 1 M glucose was added to 1 l SOB medium. |
| Stock medium | 63 g glycerol and 10 g peptone were dissolved in 500 ml $H_2O$ and sterilised in the autoclave. |
| **Buffers for cloning and agarose gel** | |
| 5x ISO Mix (3 ml) | 1.5 ml Tris HCl pH 7.5, 150 µl 1 M $MgCl_2$, 300 µl 10 mM dNTP Mix, 150 µl 1 M DTT, 750 mg PEG 8000, 100 mM NAD were filled up to 3 ml with $H_2O$. |
| Gibson master mix | 100 µl 5x ISO mix, 0.2 µl T5 exonuclease, 6.25 µl Phusion DNA polymerase and 50 µl *Taq* DNA Ligase were mixed with 218.6 µl $H_2O$. |
| 6x DNA loading buffer | 1.9 ml 80 % (v/v) glycerol and a little bit of bromophenol blue were added to 3 ml $H_2O$. The pH was adjusted with ca. 20 µl Tris HCl pH 8.8 until the solution appeared blue. |
| **Buffers for crude membranes** | |
| 50x TAE buffer | 242 g Tris base, 57.1 ml glacial acetic acid and 37.2 g EDTA were dissolved in 1 l $H_2O$. The buffer was diluted 1:50 in $H_2O$ before use. |
| Buffer K | 50 mM TEA, 250 mM sucrose and 1 mM EDTA pH 8 were dissolved in 500 ml $H_2O$. The pH was adjusted to 7.5 with acetic acid. |
| 10x PBS (phosphate buffered saline) | 80 g NaCl, 2 g KCl, 14.4 g $Na_2HPO_4 * 2H_2O$ and 2.4 g $KH_2PO_4$ were dissolved in 1 l $H_2O$ and pH was adjusted to 7.4 with NaOH. The buffer was used after 1:10 dilution in $H_2O$. |
| **Buffers for SDS-PAGE** | |
| 4x SB buffer | 10 ml 0.5 M Tris-HCl pH 6.8, 5 ml 80 % (v/v) glycerol, 1.6 g SDS and 10 mg bromophenol blue were filled up to 16 ml with $H_2O$, mixed and then filled up to 20 ml with $H_2O$. Before use, the buffer was diluted 4x with $H_2O$ and 5 % (v/v) β-mercaptoethanol was added. |
| 10x SDS running buffer | 30 g Tris Base, 144 g Glycine and 10 g SDS were dissolved in 1 l $H_2O$. Before use, the buffer was diluted 1:10 in $H_2O$. |

| Buffers for BN-PAGE | |
|---|---|
| 10x Blue native loading buffer | 25 mg Coomassie Serva Blue G were dissolved in 450 µl 250 mM aminocaproic acid supplemented with 50 % (v/v) glycerol. |
| 10x Anode buffer | 52.3 g Bis-Tris were dissolved in 500 ml $H_2O$. The buffer was diluted 1:10 in $H_2O$ before use. |
| 10x Cathode buffer I | 44.79 g tricine, 15.69 g Bis-Tris and 1 g Coomassie Serva Blue G were dissolved in 500 ml $H_2O$ and mixed over night at 4°C. The buffer was diluted 1:10 in $H_2O$ before use. |
| 10x Cathode buffer II | 44.79 g tricine, 15.69 g Bis-Tris were dissolved in 500 ml $H_2O$ and mixed over night at 4°C.<br>Before use, 192 ml $H_2O$ were mixed with 24 ml cathode buffer I (from the chamber, 1x) and 24 ml cathode buffer II (10x) |
| **Buffers for Western Blotting** | |
| 10x Transfer buffer | 30 g Tris base, 144 g glycine and 2.5 g SDS were dissolved in 1 l $H_2O$. Before use, the buffer was diluted 1:10 in $H_2O$ supplemented with a final concentration of 10 % (v/v) ethanol. |
| 10x TBS | 84 g NaCl and 30 g Tris Base were dissolved in 1 l $H_2O$. The pH was adjusted to 8.0 with HCl. The buffer was diluted 1:10 in $H_2O$ before use. |
| TBS-T | 1x TBS was supplemented with 0.05 % (v/v) Tween20. |

Table 3: Antibodies used in this study

| **Designation** | **Origin** | **Dilution (in TBS-T)** | **Clonality** | **Order** | **Manu-facturer** |
|---|---|---|---|---|---|
| α-FLAG | mouse | 1:10,000 for SDS-PAGE<br>1:5,000 for BN-Page | monoclonal | primary | Sigma |
| α-HiBiT | mouse | 1:10,000 for SDS-PAGE<br>1:5,000 for BN-Page | monoclonal | primary | Promega |
| α-Mouse DyLight 800 | goat | 1:1,000 | polyclonal | secondary | Thermo Fisher |

Table 4: List of *E. coli* and *S.* Typhimurium (*S.* T.) strains used in this study

| **Name** | **Species** | **Genotype** | **Made with plasmid** | **Source** |
|---|---|---|---|---|
| pir116 | *E. coli* | endA1 hsdR17 glnV44 (= supE44) thi-1 recA1 gyrA96 relA1 _80dlac_(lacZ)M15 _(lacZYA argF)U169 zdg-232 uidA::pir116 | - | Lab collection |
| β2163 | *E. coli* | (F-) RP4-2-Tc::Mu DdapA::(erm-pir) [KmR ErmR] | - | Lab collection |
| SB300 (WT) | *S.* T. | *Salmonella enterica* subspecies *enterica* serovar Typhimurium SL1344 | - | Lab collection |
| MIB5731 | *S.* T. | *siiF*-3xFLAG, *sipA*-NL-myc | pMIB7881 | This study |
| MIB5733 | *S.* T. | Δ*hilD*, *siiF*-3xFLAG, *sipA*-NL-myc | pMIB7881 | This study |
| MIB5735 | *S.* T. | Δ*invA*, *siiF*-3xFLAG, *sipA*-NL-myc | pMIB7881 | This study |
| MIB5737 | *S.* T. | ΔhilA, siiF-3xFLAG, *sipA*-NL-myc | pMIB7881 | This study |
| MIB5832 | *S.* T. | *siiF*G500E-3xFLAG, *sipA*-NL-myc | pMIB7890 | This study |

| | | | | |
|---|---|---|---|---|
| MIB5807 | *S*. T. | *siiF*K506L-3xFLAG, *sipA*-NL-myc | pMIB7887 | This study |
| MIB5834 | *S*. T. | Δ*invA*, *siiF*G500E-3xFLAG | pMIB7890 | This study |
| MIB5863 | *S*. T. | Δ*invA*, *siiE*::K5411HiBiT, *siiF*K506L-3xFLAG | pMIB7887 | This study |
| MIB5739 | *S*. T. | *siiE*::K5411NanoLuc | pMIB7884 | This study |
| MIB5741 | *S*. T. | Δ*hilD*, *siiE*::K5411NanoLuc | pMIB7884 | This study |
| MIB5743 | *S*. T. | Δ*invA*, *siiE*::K5411NanoLuc | pMIB7884 | This study |
| MIB5745 | *S*. T. | Δ*hilA*, *siiE*::K5411NanoLuc | pMIB7884 | This study |
| MIB5828 | *S*. T. | *siiE*::K5411NanoLuc, *siiF*G500E-3xFLAG | pMIB7890 | This study |
| MIB5799 | *S*. T. | *siiE*::K5411NanoLuc, *siiF*K506L-3xFLAG | pMIB7887 | This study |
| MIB5836 | *S*. T. | Δ*siiF*, *siiE*::K5411NanoLuc | pMIB7992 | This study |
| MIB5841 | *S*. T. | *siiF*ΔN463-M688, *siiE*::K5411NanoLuc | pMIB7994 | This study |
| MIB5849 | *S*. T. | *siiE*::K5411HiBiT | pMIB8000 | This study |
| MIB5857 | *S*. T. | *siiE*::K5411HiBiT, *siiF*G500E-3xFLAG | pMIB7890 | This study |
| MIB5861 | *S*. T. | *siiE*::K5411HiBiT, *siiF*K506L-3xFLAG | pMIB7887 | This study |
| MIB5853 | *S*. T. | Δ*siiF*, *siiE*::K5411HiBiT | pMIB8022 | This study |
| MIB5858 | *S*. T. | Δ*hilD*, *siiE*::K5411HiBiT, *siiF*G500E-3xFLAG | pMIB7890 | This study |
| MIB5851 | *S*. T. | Δ*invA*, *siiE*::K5411HiBiT | pMIB8000 | This study |
| MIB5850 | *S*. T. | Δ*hilD*, *siiE*::K5411HiBiT | pMIB8000 | This study |
| MIB5852 | *S*. T. | Δ*hilA*, *siiE*::K5411HiBiT | pMIB8000 | This study |
| MIB5866 | *S*. T. | *siiE*::K5411HiBiT, *siiF*K506L | pMIB7887 | This study |
| MIB3877 | *S*. T. | *sipA*-3xFLAG-HiBiT | - | Lab collection |
| MIB4841 | *S*. T. | Δ*hilD* | - | Lab collection |
| SB1751 | *S*. T. | Δ*invA* | - | Lab collection |
| MIB5747 | *S*. T. | ΔSPI4 | pMIB7885 | This study |
| MIB5749 | *S*. T. | Δ*invA*, ΔSPI4 | pMIB7885 | This study |
| MIB5835 | *S*. T. | Δ*siiF* | pMIB7992 | This study |
| MIB5826 | *S*. T. | Δ*hilD*, *sipA*-3xFLAG-HiBiT | pMIB6645 | This study |
| MIB5825 | *S*. T. | Δ*invA*, *sipA*-3xFLAG-HiBiT | pMIB6645 | This study |
| MIB5821 | *S*. T. | ΔSPI4, *sipA*-3xFLAG-HiBiT | pMIB6645 | This study |
| MIB5822 | *S*. T. | ΔSPI4, Δ*invA*, *sipA*-3xFLAG-HiBiT | pMIB6645 | This study |

Table 5: List of plasmids used in this study

| Name | Insert | Description | Source |
|---|---|---|---|
| pNL1.1 | - | plasmid encoding NanoLuc | Cat. #N1001, Promega |
| pMIB6645 | - | *sipA*-3xFLAG-HiBiT | Lab collection |

| | | | |
|---|---|---|---|
| pMIB7881 | *siiF*-3xFLAG | *siiF*-3xFLAG ±1000 bp in pSB890<br>3xFLAG at the C-terminus of SiiF<br>Made by Gibson Assembly of PCR products of the following three primer/template pairs:<br>1. Insert: gib_890_ssiF_a_f + gib_FLAG_siiF_b_r from SB300 chromosomal DNA;<br>2. Insert: gib_FLAG_siiF_c_f + gib_890_siiF_d_r from SB300 chromosomal DNA;<br>3. Plasmid: gib_uni_890_f2 + gib_uni_890_r2 from pSB890 (p890) | This study |
| pMIB7890 | *siiF*G500E-3xFLAG | *siiF*G500E-3xFLAG ±1000 bp in pSB890 (G500E mutation in Walker A motif of SiiF, 3xFLAG at the C-terminus of SiiF). Made by QC using plasmid pMIB7881 and primer QC_SiiF_G500E_f and QC_SiiF_G500E_r | This study |
| pMIB7887 | *siiF*K506L-3xFLAG | *siiF*K506L-3xFLAG ±1000 bp in pSB890 (K506L mutation in Walker A motif of siiF, 3xFLAG at the C-terminus of siiF). Made by QC using plasmid pMIB7881 and primer QC_SiiF_K506L_f and QC_SiiF_K506L_r | This study |
| pMIB7884 | *siiE*::K5411NanoLuc | *siiE*::K5411NanoLuc ±1000 bp in pSB890. Insertion of NanoLuc inside *siiE* at position K5411. Made by Gibson Assembly in two steps of PCR products of the following primer/template pairs:<br>Step 1: Insertion of siiEK5411 ±1000 bp in pSB890<br>1. Insert: gib_890_Ig53_a_f + gib_890_Ig53_d_r2 from SB300 chromosomal DNA<br>2. Plasmid: gib_uni_890_f2 + gib_uni_890_r2 from pSB890 (p890).<br>Step 2: Insertion of NanoLuc at position K5411 in pSB890-siiE±1000 bp<br>1. Insert: gib_siiE_Nluc_f + gib_siiE_Nluc_r from pNL1.1<br>2. Plasmid: gib_890_Ig53_b_r + gib_Nluc_Ig53_c_f from pSB890-siiE±1000bp (from Step1) | This study |
| pMIB7992 | Δ*siiF* | Δ*siiF* ±1000 bp in pSB890. Made by Gibson Assembly of PCR products of the following three primer/template pairs:<br>1. Insert: gib_890_dsiiF_a_f + gib_dsiiF_b_r from SB300 chromosomal DNA;<br>2. Insert: gib_dsiiF_c_f + gib_890_dsiiF_d_r from SB300 chromosomal DNA;<br>3. Plasmid: gib_uni_890_f2 + gib_uni_890_r2 from pSB890 (p890) | This study |
| pMIB7994 | *siiF*ΔN463-M688 | *siiF*ΔN463-M688 ±1000 bp in pSB890 (deletion of ATPase in *siiF*). Made by Gibson Assembly of PCR products of the following three primer/template pairs:<br>1. Insert: gib_890_dATPsiiF_a_f + gib_dATPsiiF_b_r from SB300 chromosomal DNA | This study |

| | | | |
|---|---|---|---|
| | | 2. Insert: gib_dATPsiiF_c_f + gib_890_dATPsiiF_d_r from SB300 chromosomal DNA<br>3. Plasmid: gib_uni_890_f2 + gib_uni_890_r2 from pSB890 (p890) | |
| pMIB8000 | *siiE*::K5411HiBiT | *siiE*::K5411HiBiT ±1000 bp in pSB890. Insertion of HiBiT inside *siiE* at position K5411. Made by Gibson Assembly in two steps of PCR products of the following two primer/template pairs:<br>Step 1: Insert<br>1. gib_890_HiBiT_a_f + gib_HiBit_Ig53_b_r from SB300 chromosomal DNA;<br>2. gib_HiBit_Ig53_c_f + gib_890_HiBiT_d_r from SB300 chromosomal DNA;<br>and subsequently PCR products from Step 1 were used as templates for second PCR with:<br>gib_890_HiBiT_a_f + gib_890_HiBiT_d_r<br>Step 2: Plasmid: gib_uni_890_f2 + gib_uni_890_r2 from pSB890 | This study |
| pMIB8022 | Δ*siiF*, *siiE*::K5411HiBiT | Δ*siiF* ±1000bp with *siiE*::HiBiT in pSB890 (*siiE*::K5411HiBiT in the region upstream of *siiF*). Made by Gibson Assembly of PCR products of the following three primer/template pairs:<br>1. Insert: gib_890_dsiiF_a_f + gib_dsiiF_b_r from MIB5849 (*siiE*::K5411HiBiT) chromosomal DNA;<br>2. Insert: gib_dsiiF_c_f + gib_890_dsiiF_d_r from MIB5849 (*siiE*::K5411HiBiT) chromosomal DNA;<br>3. Plasmid: gib_uni_890_f2 + gib_uni_890_r2 from pSB890 (p890) | This study |
| pMIB7885 | Δ*siiABCDEF* | Δ*siiABCDEF* ±1000 bp in pSB890, Made by Gibson Assembly of PCR products of the following two template pairs:<br>1. Insert: gib_890_SPI4_a_f_PlanB + gib_890_SPI4_d_r_PlanB from two PCR products amplified chromosomal DNA (SB300) made with gib_890_SPI4_a_f + gib_dSPI4_b_r and gib_dSPI4_c_f + gib_890_SPI4_d_r2<br>2. Plasmid: gib_uni_890_f2 + gib_uni_890_r2 from pSB890 (p890) | This study |

Table 6: List of primers used in this study

| Primer name | Sequence (5‘ to 3‘) |
|---|---|
| gib_uni_890_f2 | CAAGCTCAATAAAAAGCCCCAC |
| gib_uni_890_r2 | CAAGAGGGTCATTATATTTCGCG |
| gib_890_ssiF_a_f | CGCGAAATATAATGACCCTCTTGTCAAGGGTGATGTTACTACTGGCGC |
| gib_FLAG_siiF_b_r | ATCGATGTCATGATCTTTATAATCACCGTCATGGTCTTTGTAGTCCATTAATAATTTATCCGGAGAAC |
| gib_FLAG_siiF_c_f | GATTATAAAGATCATGACATCGATTACAAGGATGACGATGACAAATAAAATAAGCAGCGCTTGTCGCTG |

| | |
|---|---|
| gib_890_siiF_d_r | GTGGGGCTTTTTATTGAGCTTGATCTCTTTCGCATACCAGG CAGGAC |
| QC_SiiF_G500E_f | ACGTGTCGCGGTGGTAGAAGAATGCGGAGCAGGAAAAAGC |
| QC_SiiF_G500E_r | TTTCCTGCTCCGCATTCTTCTACCACCGCGACACGTTGCC |
| QC_SiiF_K506L_f | GGCGAATGCGGAGCAGGATTAAGCTCATTACTGGGAATGC TATCTGGC |
| QC_SiiF_K506L_r | GCATTCCCAGTAATGAGCTTAATCCTGCTCCGCATTCGCCT ACCACC |
| gib_890_Ig53_a_f | TTATTCCGCGAAATATAATGACCCTCTTGACGCCGCCAAAT GCTCCGGTC |
| gib_890_Ig53_d_r2 | CCACCGCGGTGGGGCTTTTTATTGAGCTTGAACAGAGTTCA CCGCGCG |
| gib_siiE_Nluc_f | CCGTCTGCGGCGGAAGAAAGCGTGGTGAAGATGGTCTTCA CACTCGAAGATTTCG |
| gib_siiE_Nluc_r | GTTTAACAATGTAATACTATAGGCTGTCACCGCCAGAATGC GTTCGCAC |
| gib_890_Ig53_b_r | CCCAACGAAATCTTCGAGTGTGAAGACCATCTTCACCACGC TTTCTTCCGCCGC |
| gib_Nluc_Ig53_c_f | GGCTGGCGGCTGTGCGAACGCATTCTGGCGGTGACAGCCT ATAGTATTACATTG |
| gib_890_dsiiF_a_f | TGTTATTCCGCGAAATATAATGACCCTCTTGCTTTACGCCAG GTACACCG |
| gib_dsiiF_b_r | CCACCTGATAACAGCGACAAGCGCTGCTTATTAAGTAAACC CCCTCACCC |
| gib_dsiiF_c_f | TCACCTTTGGGTGAGGGGGTTTACTTAATAAGCAGCGCTTG TCGC |
| gib_890_dsiiF_d_r | CCACCGCGGTGGGGCTTTTTATTGAGCTTGTCTTTCGCATA CCAGGCAGG |
| gib_890_dATPsiiF_a_f | TATTCCGCGAAATATAATGACCCTCTTGCGGGCAAAAAATA AAGTTGG |
| gib_dATPsiiF_b_r | CCACCTGATAACAGCGACAAGCGCTGCTTATTGCACTTTGA TATTGACTG |
| gib_dATPsiiF_c_f | CCGGCATTACAGTCAATATCAAAGTGCAATAAGCAGCGCTT GTCGC |
| gib_890_dATPsiiF_d_r | CCGCGGTGGGGCTTTTTATTGAGCTTGCAAATGGAGGTTTA CGGTGC |
| gib_890_HiBiT_a_f | TTCCGCGAAATATAATGACCCTCTTGACGCCGCCAAATGCT CCGGTC |
| gib_HiBit_Ig53_b_r | GCTAATCTTCTTGAACAGCCGCCAGCCGCTCACCTTCACCA CGCTTTCTTCCGCCGC |
| gib_HiBit_Ig53_c_f | GTGAGCGGCTGGCGGCTGTTCAAGAAGATTAGCGTGACAG CCTATAGTATTACATTG |
| gib_890_HiBiT_d_r | GCGGTGGGGCTTTTTATTGAGCTTGATCAATATCGACGTCA TCCT |
| gib_890_SPI4_a_f | GTTATTCCGCGAAATATAATGACCCTCTTGATGGCCAGCAG AGGC |
| gib_dSPI4_b_r | ACCTGATAACAGCGACAAGCGCTGCTTATTGTTGTCTCCTG ATATTACATTGTG |
| gib_dSPI4_c_f | TTTATTCACAATGTAATATCAGGAGACAACAATAAGCAGCG CTTGTCGC |
| gib_890_SPI4_d_r2 | GCCACCGCGGTGGGGCTTTTTATTGAGCTTGCGTTTATAGT CAGCGCGGG |
| gib_890_SPI4_a_f_PlanB | GTTATTCCGCGAAATATAATGACCCTCTTGCCGGAAGTACG CTATATGCC |
| gib_890_SPI4_d_r_PlanB | GCCACCGCGGTGGGGCTTTTTATTGAGCTTGGAGCATAGA AAACGCTGGCC |

| | |
|---|---|
| seq_up_siiF_f | GTCTGAGTAGTGACGCCAG |
| seq_down_siiF_r | AATGGCAAGTGGAATAGCCC |
| seq_up_siiF_K506L_f | GTCAATATCAAAGTGCAATGGCG |
| seq_up_siiF_K506L_f_2 | CAGTATGATGCTCAATCTCC |
| seq_up_NLuc_f | GGGGAATTCACAGCAATCTGC |
| seq_down_NLuc_r | GTTCACAATATCCGCCGAGG |
| seq_dsiiF_f | CATTCTCAGTCGATCACTCC |
| seq_dsiiF_f2 | GTAAGAGGAAAGACCG |
| seq_dsiiF_r | CCACCGGTTATCTCAACGC |
| seq_dATPsiiF_f | AAGGGTGATGTTACTACTGGCG |
| seq_dATPsiiF_r | AATGGCCGATGGTGCTGACC |
| seq_up_siiA_f | CGATACCTATTATTGGGGAGG |
| seq_down_siiF_r | GCCTTGCGCACCATC |
| seq_SipA_HiBiT_f | TAGCGATATTGACAAGCACCC |
| sipA_seq_r | TCAGCGTAAAGATCCTCAACC |
| seq_SipA_L632_f | CTGACCAGGCTAAAAGGGG |

## 2.2 Cloning and allelic exchange

### 2.2.1 Gibson Assembly

Gibson Assembly is a single reaction, one-step isothermal method used for assembly of multiple overlapping DNA fragments. It can be used for cloning of multiple inserts into a plasmid (Gibson et al. 2009). The vector (pSB890) and inserts were amplified by PCR with Q5 Hot Start High-Fidelity DNA Polymerase and Gibson primers. Gibson primers are designed with an overhang (20 - 30 bp), that overlaps with the respective sequence of the other insert or vector (Table 6). The PCR products were analysed on a 1 or 2 % agarose gel in TAE buffer and the amplified vector was digested with DpnI for at least 1 h at 37°C.

The Gibson Assembly was performed for 1 h at 50°C with 12.5 µl Gibson master mix and 3 or 5 µl of the respective PCR fragment. Then, 5 µl of the newly assembled plasmid were used for standard heat shock transformation into competent pir116. The next day, colony PCR was performed to identify clones with the correct length of the insert. Plasmids were isolated using the QIAprep Spin Miniprep Kit (Qiagen) and sent for sequencing analysis (Eurofins Genomics).

### 2.2.2 QuikChange site-directed mutagenesis

For the non-secreting SPI-4 strain, a point mutation in the Walker A motif of the nucleotide binding domain (NBD) of SiiF (Gerlach et al. 2009) was introduced by

QuikChange (QC) mutagenesis (Agilent Technologies). QC primers (Table 6) were designed with a rich GC content and a desired mutation in the middle of the primer. The PCR reaction setup is shown in Table 7.

Table 7: KOD QuikChange reaction setup

| Component | 50 µl Reaction |
|---|---|
| 10x KOD Reaction Buffer | 5 µl |
| 2 mM dNTPs | 5 µl |
| forward QC primer | 1.25 µl |
| reverse QC primer | 1.25 µl |
| template DNA | 3 µl |
| KOD DNA Polymerase | 0.5 µl |
| 25 mM $MgSO_4$ | 4 µl |
| Nuclease-free Water | 30 µl |

1 µl DpnI was added to the PCR product and incubated for 1 h at 37°C (to digest the template plasmid). Then, 5 µl of the new plasmid were transformed by standard heat shock transformation into competent pir116. QlAprep Spin Miniprep Kit (Qiagen) was used for the extraction of the plasmids of different strains, which were then sent for sequencing analysis (Eurofins Genomics) to identify positive mutants.

### 2.2.3 Allelic exchange

The allelic exchange protocol was used to delete genes, insert tags or point mutations on the chromosomal level of *Salmonella*. The suicide plasmid pSB890 has a tetracycline resistance and the counter selection gene *sacB*. Gibson Assembly (2.2.1) was used for cloning the plasmid (Table 5) containing the mutated gene and ±1000 bp of the flanking regions up- and downstream of the target gene. These are identical to the chromosomal sequence and ensure homologous recombination. The plasmid was introduced into *E. coli* β2163 donor strains by electroporation. Since β2163 needs DAP, strains were grown o/n in LB/Tet/DAP and the recipient *Salmonella* strain was grown in LB/Strep. The next day, 900 µl of the donor and recipient culture were mixed in a 2 ml tube, centrifuged at 6,000 rpm (Eppendorf MiniSpin, rotor F-45-12-11), 2 min, RT and washed with 1 ml LB/DAP to remove residual antibiotics. The culture was centrifuged again and the supernatant was removed by inverting the tube. The

remaining drop of supernatant was used for resuspending the cell pellet and 30 µl of the suspension were spotted on a LB/DAP agar plate without antibiotics and incubated o/n at 37°C to enable mating, that is, the transfer of the plasmid from β2163 to *Salmonella* cells via conjugation. The next day, cells were scraped off, resuspended in 1 ml LB and 100 µl were plated on a selective LB/Strep/Tet plate. Since *Salmonella* cannot replicate the pSB890 plasmid with the R6K origin, only strains that have integrated the entire plasmid (with the Tet resistance) into the chromosome through homologous recombination can survive in presence of the selective antibiotic. After the first homologous recombination, strains are also called merodiploids and two different merodiploids were grown in 5 ml LB/Strep for 24 hours. Then, 1.5 µl of the culture were diluted in 1 ml LB (~$10^{-3}$) and 100 µl were plated on a counter selective LB/Strep/sucrose plate and incubated o/n at 30°C. The counter selective gene *sacB* encodes levansucrase that converts sucrose to cytotoxic levan. Thus, only strains that have lost the integrated plasmid by a second homologous recombination event can grow on sucrose plates. As a further confirmation, colonies from the sucrose plates were streaked out on LB/Strep and LB/Tet plates in that order and only colonies that have grown on LB/Strep but not on LB/Tet plates were further analysed. The second homologous recombination or looping out event can either result in the wild type allele or the mutant. Therefore, a colony PCR was performed with an expected PCR product that is smaller or larger than wild type for a gene deletion or insertion, respectively (Hurley 2018). The PCR products were further sent for sequencing analysis (Eurofins genomics) to confirm the presence of single point mutations.

## 2.3 BN-PAGE and SDS-PAGE

### 2.3.1 Crude membranes

Bacterial cultures were grown in 10 ml LB 0.3 M NaCl medium in 50 ml Falcon tubes for 5 h under conditions as described in (2.1.1).

The $OD_{600}$ was measured and, if not mentioned otherwise, bacterial cell pellets of 8 ODU were harvested by centrifugation at 10,000 x *g*, 5 min, 4°C. All further

steps were performed on ice. The supernatant was removed and cell pellets were treated further for crude membrane extraction or stored at -20°C.

The day before, 2 ml screw cap tubes were prepared with 0.5 ml glass beads (150 - 212 µm, acid-washed, Sigma-Aldrich) and stored in the fridge to precool. The bacterial cell pellet was resuspended in 750 µl buffer K with additives, added to the glass beads in screw cap tubes and incubated for 30 min on ice. Then, the samples were bead milled for 2 min at continuous mode with a SpeedMill PLUS (Analytik Jena). After centrifugation at 1,000 x *g*, 1 min, 4°C the supernatant (~ 400 µl) was transferred to a fresh 1.5 ml tube and 1 ml buffer K without additives was added to the beads. Again, the screw cap tubes were centrifuged at 1,000 x *g*, 1 min, 4°C and the supernatant was transferred to the same 1.5 ml tube as before. The 1.5 ml tube was centrifuged at 10,000 x *g*, 10 min, 4°C to separate supernatant from remaining beads, cell debris and unbroken cells, and 1.3 ml of the supernatant were transferred to ultracentrifugation tubes (Beckman). The samples were centrifuged at 50,000 rpm, 50 min, 4°C in an ultracentrifugation (Beckmann Coulter, TLA 55 rotor) to isolate crude membranes. Subsequently, the supernatant was aspirated and the membrane pellets were directly subjected to further treatment for BN-PAGE.

### 2.3.2 BN-PAGE

The Blue Native (BN)-PAGE allows the investigation of membrane proteins and membrane protein complexes in their native protein conformation (Zilkenat et al. 2017). Membrane proteins are extracted gently through nonionic detergents. Hydrophobic regions of the extracted membrane proteins are bound by the water-soluble blue dye Coomassie G, which leads to a charge shift of the proteins. This allows the electrophoretic separation of the protein complexes depending on their size on a gradient gel (Schägger and von Jagow 1991).

The running-chamber was set up with the Invitrogen NativePAGE 4 - 16 % Protein Gel and filled with anode buffer and cathode buffer I, respectively, and placed in a 4°C cold room.

Crude membrane pellets from 8 ODU were resuspended in 90 µl PBS and solubilised by pipetting 40 - 80 times up and down. 10 µl of 10 % (w/v) detergent lauryl maltose neopentyl glycol (LMNG) (Anatrace, Maumee, U.S.) were added to the sample (final concentration of 1 % (w/v)) and membrane proteins were solubilised for 1 h at 4°C with 500 rpm shaking. Unsolubilised material was pelleted by centrifugation at 20,000 x *g*, 30 min, 4°C. Then, 45 µl and 30 µl of the supernatant were transferred into new 1.5 ml tubes for BN-PAGE and SDS-PAGE (2.3.3), respectively. 5 µl from the 10x BN loading buffer with Coomassie were added to the 45 µl solubilised membrane proteins into the 1.5 ml tube and mixed by pipetting up and down. Per sample, 20 µl were loaded into the well of the gel. As a size reference 8 µl of Native Mark unstained protein standard was used.

After the first step of electrophoresis ran at 130 V for 50 - 55 min, the cathode buffer I was replaced by cathode buffer II and second step of electrophoresis ran at 300 V for 1.5 h (until Coomassie runs out of the gel). After the run, the wells and the dark blue lower part of the gel were cut off and the gel was equilibrated in SDS running buffer for 20 - 30 minutes. When a native marker was used, the marker lane was cut off and stained with Jove Coomassie.

The Western Blot was performed under wet conditions as described below (2.3.4). After the transfer onto a PVDF membrane by Western Blotting, the membrane was washed several times before blocking with 100 % methanol to remove blue Coomassie residuals until the membrane was completely white again.

**Supernatant on the BN-PAGE**

In order to detect SiiE secreted into culture medium, 2 ml of supernatant were concentrated using an Amicon Ultra-4 10k Filter. Subsequently, 20 µl of the concentrated supernatant were mixed with 2 µl of the BN loading buffer and the sample was loaded on the BN-PAGE as described above (2.3.2).

### 2.3.3 SDS-PAGE

10 µl of 4x SB buffer were added to the 30 µl solubilised membrane proteins prepared for SDS-PAGE (2.3.2). The samples were heated to 50°C for 10 min, briefly centrifuged (10 s) and 20 µl were loaded on SERVAGel TG PRiME 8 - 16 % or 4 - 20 % electrophoresis gel, as indicated. Precision Plus Protein All Blue standards was used as a size reference. The electrophoresis ran at 100 V for 15 min followed by 210 V for 85 min in 1x SDS running buffer.

When whole cells were used for SDS-PAGE, 0.5 ODU cells were pelleted in a 1.5 ml tube (10,000 x *g*, 2 min, 4°C) and supernatant was removed. The cell pellet was resuspended in 75 µl of 1x SB buffer and heated for 10 min at 50°C. Then, the samples were cooled down to RT for approximately 10 min, vortexed for 30 s and 15 µl were loaded on SERVAGel TG PRiME 8 - 16 % or 4 - 20 % electrophoresis gel, as indicated. Electrophoresis ran at 100 V for 15 min followed by 210 V for 85 min in 1x SDS running buffer.

### 2.3.4 Western Blotting

For transferring the proteins from the gel to the membrane the electrophoretic chamber Criterion Blotter (Bio-Rad) was used for Western blotting under wet conditions. The polyvinylidene difluoride (PVDF) membrane (Bio-Rad) was activated in 100 % ethanol. Then, the activated PVDF membrane, SDS or BN gel and Whatman-Papers were equilibrated in 1x transfer buffer and the transfer sandwich was assembled carefully without air bubbles. The cassette was placed in the transfer tank filled with transfer buffer and an ice block was placed in the tank.

The transfer was performed at 35 V for 3.5 h at 4°C. After the transfer, unspecific binding sites on the membrane were blocked with 10x BlueBlock PF diluted 1:10 in TBS for 1 h at RT. Membranes were washed once in TBS-T and incubated with 10 ml TBS-T primary antibody solution (Table 3) for 1 h, at RT or overnight at 4°C. After the primary antibody's incubation, the membranes were washed three times for 15 min in TBS-T and incubated with 10 ml TBS-T secondary antibody solution (Table 3) for 1 h at RT. Finally, the membranes were washed again three

times with TBS-T and transferred to TBS buffer. Membranes were scanned with a LI-COR Odyssey system (ODY-3191) and images were analysed with Image Studio 2.1 (LI-COR).

## 2.4 NanoLuc luciferase assay

Developed in 2012, NanoLuc (Nluc) is a small 19.1 kDa luciferase enzyme derived from the deep-sea shrimp *Oplophorus gracilirostris.* Nluc reacts with the substrate furimazine, a derivative from coelenterazine, and produces luminescence (reviewed in England et al. 2016).

Promega has developed the splitted HiBiT-LgBiT system. HiBiT is a small 11 amino acid peptide fragment of the NanoLuc luciferase. It binds with high affinity to the larger subunit LgBiT (that is NanoLuc luciferase missing the HiBiT fragment) (Schwinn et al. 2018; Westerhausen et al. 2020). The HiBiT-LgBiT complex reacts with furimazine and releases luminescence (Lee 2017).

Table 8: Promega protein detection systems

| Product | Components | Ratio | Supplier |
|---|---|---|---|
| Nano-Glo Luciferase Assay System | Nano-Glo Luciferase Assay Buffer<br>Nano-Glo Luciferase Assay Substrate | substrate-buffer: 1:50 | Promega (N1110) |
| Nano-Glo Extracellular NanoLuc Substrate | Nano-Glo Extracellular NanoLuc Substrate<br>(prototype, provided from Promega through personal communication) | substrate-buffer: 1:50 | Promega (prototype R&D USA) |
| Nano-Glo HiBiT Extracellular Detection System | Nano-Glo HiBiT Extracellular Buffer<br>Nano-Glo HiBiT Extracellular substrate<br>LgBiT protein | substrate-buffer: 1:50<br>LgBiT-buffer: 1:100 | Promega (N2420) |
| Nano-Glo Live Cell Assay System | Nano-Glo LCS Dilution Buffer<br>Nano-Glo Live Cell Substrate | substrate-buffer: 1:20 | Promega (N2012) |
| DrkBiT peptide | DrkBiT<br>(provided from Promega through personal communication) | DrkBiT-buffer: 1:1,000 | Promega |

### 2.4.1 SiiE secretion assay

NanoLuc and HiBiT were inserted chromosomally into SiiE upstream of BIg53, at amino acid position K5411 (Figure 5a, Figure 6a).

**SiiE secretion assay, end point**

This assay was established to assess SiiE secretion into the culture medium, SiiE retention at the bacterial cell surface and to measure SiiE expression level in bacterial cells.

*Salmonella* strains were grown o/n, subcultured the next day and grown for another 5 h under SPI-4 inducing conditions (2.1.1). $OD_{600}$ was measured and 0.5 ODU were transferred into a 1.5 ml tube and centrifuged at 10,000 x *g*, 2 min, 4°C. Supernatant was transferred into a new 1.5 ml tube and kept on ice.

If not stated otherwise, bacterial cells were washed gently twice with precooled PBS to remove all residual secreted SiiE and resuspended in PBS with the same volume used to harvest 0.5 ODU. Bacterial cells in PBS are referred to as whole cells.

25 µl from the supernatant and whole cells were transferred into a 384-well plate. The experiment was performed with three technical replicates per sample.

The respective Nano-Glo Buffer Substrate mix or Nano-Glo HiBiT Extracellular Buffer Substrate LgBiT mix (Table 8) was prepared. 25 µl of the buffer substrate mix were added to each sample. A multichannel pipette was used to ensure same reaction time for all samples. 25 µl buffer substrate mix were added to 25 µl LB 0.3 M NaCl or 25 µl PBS, respectively, to measure unspecific background level.

After 10 min reaction time, the 384-well plate was placed into the Tecan Spark reader for luminescence measurement with the following parameters: shaking orbital: 5 s, shaking amplitude: 2.5 mm, attenuation: automatic, settle time: 0 ms, integration time: 1000 ms. Negative luminescence after subtracting of the background control (blank) was set as 0 and is not shown on the logarithmic scale. The same protocol was also used to quantify T3SS-1 SipA-HiBiT secretion into culture supernatant.

**Bacterial cells and supernatant**

To simultaneously assess expression and secretion, instead of separating supernatant from bacterial cells by centrifugation, 25 µl from the subculture (bacterial cells + supernatant) were transferred directly into a 384-well plate.

**SiiE secretion kinetic**

This assay was established to assess the secretion of SiiE continuously by growth in 96-well plate inside a Tecan Spark plate reader.

For measuring continuous SiiE secretion, 1 ml from the o/n cultures was transferred into a 1.5 ml tube, centrifuged at 6,000 rpm, 2 min, RT and washed with PBS to remove the supernatant with secreted SiiE. Then, bacteria were subcultured to a target $OD_{600}$ of 0.1 in 125 µl (100 µl prewarmed LB 0.3 M NaCl medium + 25 µl Nano-Glo HiBiT Buffer Substrate LgBiT mix) in a prewarmed 96-well plate. The 96-well plate was placed into a humidity cassette in the prewarmed Tecan Spark plate reader at 37°C. Luminescence measurement was performed with the following parameters: Mode: kinetic, interval time: 5 min, shaking orbital: 5 s, shaking amplitude: 2.5 mm, attenuation: automatic, settle time: 0 ms, integration time: 200 ms.

Absorbance measurements were performed at $OD_{600}$ with the following parameters: number of flashes 10, settle time: 50 ms.

## 2.5 Cell Culture

The immortal epithelial cell line HeLa was derived from a cervical adenocarcinoma from Henrietta Lakes in 1951. HeLa cells used in this study were obtained from lab stocks (AG Wagner, Sektion für Zelluläre und Molekulare Mikrobiologie, Tübingen) (Table 9). HeLa-LgBiT is a cell line stably expressing LgBiT protein, which was generated in a previous study (Westerhausen et al. 2020).

Care must be taken concerning reproducibility in cell culture experiments between laboratories. Cancer cell lines like HeLa cells exhibit genetic changes during passaging which leads to genome instability and proteomic heterogeneity (Tang 2019).

Madin-Darby Canine Kidney (MDCK) cells were derived from the kidney of an adult female cocker spaniel in 1958. MDCK cells are reported to form a polarised monolayer with tight junctions that separate the apical side from the basolateral side (Gerlach et al. 2007b; Dukes et al. 2011). In this study the parental cell line MDCK (NBL-2) obtained from CLS GmbH was used (Table 9).

Table 9: Cell lines used in this study

| Cell line | Description | Medium | Source |
|---|---|---|---|
| HeLa | Epithelial cell line derived from a cervical adenocarcinoma (*Homo sapiens*) | DMEM (Gibco)<br>10 % (v/v) Foetal Bovine Serum (FBS) (Gibco)<br>1 % (v/v) 200 mM L-Glutamine (Gibco) | Lab collection |
| HeLa-LgBiT | HeLa cells stably expressing LgBiT protein | Same as for HeLa | Lab collection (Westerhausen et al. 2020) |
| MDCK (NBL-2) | Epithelial cell line derived from kidney cells from adult cocker spaniel (Dukes et al. 2011) | MEM (Gibco)<br>10 % (v/v) Foetal Bovine Serum (FBS) (Gibco)<br>1 % (v/v) 200 mM L-Glutamine (Gibco)<br>1 % (v/v) non-essential amino acids (NEAA) (Gibco) | CLS GmbH |

Table 10: Media and materials used for cell culture

| Product | Supplier |
|---|---|
| DMEM (4.5 g/l D-Glucose, L-Glutamine, no Pyruvate) | Gibco |
| MEM (+Earle's Salts, no L-Glutamine) | Gibco |
| Foetal Bovine Serum (FBS) | Gibco |
| L-Glutamine 200 mM (100x) | Gibco |
| Non-essential amino acids (NEAA) | Merck Biochrom |
| Hank's Balanced Salt Solution (HBSS) | Sigma-Aldrich |
| 10,000 Units/ml Penicillin / 10,000 µg/ml Streptomycin | Gibco |
| PBS pH 7.2 (1x) (no $CaCl_2$, no $MgCl_2$) | Gibco |
| PBS-T | PBS supplemented with 0.05 % (v/v) Tween 20 |
| 0.05 % Trypsin-EDTA (1x) | Gibco |
| 0.25 % Trypsin-EDTA (1x) | Gibco |
| Freezing medium | 40 % (v/v) culture medium<br>10 % (v/v) FBS<br>50 % (v/v) DMSO |
| T25, T75, T175 Flasks | Cellstar Greiner Bio-One |
| 24-well plate | Greiner Bio-One |
| 96-well plate, white, glass bottom | Thermo Fisher Scientific-Nunclon 96 Flat White |

### 2.5.1 Cultivation of HeLa, HeLa-LgBiT and MDCK (NBL-2) cells

HeLa cells were used for the invasion assay (Gerlach et al. 2007b; Gerlach et al. 2008) and HeLa-LgBiT cells for the SipA-HiBiT injection assay (Westerhausen et al. 2020). The parental MDCK cell line (NBL-2) was used to generate a polarised monolayer of MDCK cells for the invasion assay (Gerlach et al. 2008) and adhesion assay (Gerlach et al. 2007b) (data not shown). In general, basic cell

culture procedures for cultivation of MDCK (NBL-2) cells resemble those for HeLa or HeLa-LgBiT cells. Certain differences are clearly mentioned (Table 9).

**Starting a culture**

The cryotube was thawed by rapid agitation in a 37°C water bath. The cell suspension was transferred into a 15 ml Falcon tube containing 9 ml of the respective cell culture medium (Table 9). The cell suspension was centrifuged at 300 x *g*, 5 min, RT and supernatant was removed. The cells were resuspended in fresh cell culture medium, transferred into a T25 or T75 cell culture flask and grown in a 37°C incubator with humidified atmosphere of 5 % (v/v) $CO_2$. Cell morphology and growth were monitored using an inverted microscope.

**Subculturing / passaging**

The cells were passaged at a confluency of 80 - 90 %. The medium was removed and the cells were washed gently with sterile PBS (to remove residual serum that contains inhibitors). For HeLa and HeLa-LgBiT cells, 1.5 ml of 0.05 % (v/v) Trypsin EDTA (Table 10) were added to the cells and incubated for approximately 1 min in the cell culture incubator until cells were detached. Since MDCK cells are more adherent than HeLa cells, 1.5 ml of 0.25 % (v/v) Trypsin EDTA (Table 10) were used and incubation time was prolonged up to 10 min, until cells were completely detached. Trypsinisation was stopped by adding the respective cell culture medium (Table 9). Cells were splitted in a new flask and/or counted in the hemocytometer (Neubauer counting chamber). Cell culture medium was changed every three days to replenish nutrients.

**Freezing cells**

2 x $10^6$ cells were transferred into a 15 ml Falcon tube and centrifuged at 300 x *g*, 10 min, RT. The supernatant was aspirated, cells were resuspended in 1 ml of freezing medium (Table 10) and transferred into a cryovial. The cryovial was first placed in the -80°C freezer for one day before transfer into the liquid nitrogen tank.

### 2.5.2 SipA-HiBiT injection assay

HeLa-LgBiT cells were seeded into a white 96-well plate with glass bottom at a density of 1 x $10^4$ cells per well in 100 µl cell culture medium (Table 9) 24 h before the actual experiment. *Salmonella* was grown overnight and subcultured the next day for 3.5 h (2.1.1). Then, 2 ml of the subculture were transferred into a 2 ml tube and centrifuged at 6,000 x *g*, 2 min, RT. The supernatant was decanted by inverting the tube and cells were washed two times with prewarmed HBSS and subsequently resuspended in 1.5 ml HBSS. $OD_{600}$ was measured and adjusted to $OD_{600}$ of 0.2 which corresponds to approximately 3 x $10^8$ bacterial cells / ml (Geymeier 2011).

For infection, a MOI (multiplicity of infection) of 50 was used. It was estimated that HeLa-LgBiT cells duplicated within 24 h leading to 2 x $10^4$ cells per well.

The inoculum was prepared in 100 µl HBSS per well for each strain and experiments were performed with technical triplicates. The inoculum was kept at 37°C in the thermoblock until infection. DrkBiT (Table 8) was added at a ratio 1:1,000 prior to infection. DrkBiT is a membrane impermeable peptide that binds to extracellular LgBiT. The complex has no Nluc activity, thus DrkBiT reduces the background signal.

Previously seeded HeLa-LgBiT cells were washed gently two times with prewarmed PBS. PBS was aspirated completely and 100 µl of the prepared inoculum were added to each well. The plate was centrifuged for 5 min, 300 x *g*, RT for synchronising the infection. For the kinetic measurement, 25 µl of the Nano-Glo Live Cell Buffer (LCS) and Substrate (ratio 1:20) (Table 8) were added to each well. The 96-well plate was placed into a humidity cassette in the 37°C prewarmed Tecan Spark reader with a kinetic measurement for 3 hours. The following parameters were used: interval time: 5 min, shaking orbital: 5 s, shaking amplitude: 2.5 mm, attenuation: automatic, settle time: 0 ms, integration time: 200 ms. As a control for the background luminescence level, 100 µl HBSS and 25 µl Nano-Glo LCS Buffer Substrate mix were also added to a well with HeLa-LgBiT cells. This value was subtracted from the luminescence values of infected cells. Negative luminescence after subtracting of the background control (blank) was set as 0 and is not shown on the logarithmic scale.

### 2.5.3 Invasion assay of HeLa cells

Protocol adapted from Gerlach et al. 2008; Wagner et al. 2011; Wagner et al. 2014.

24 h before the experiment, HeLa cells were seeded at a density of 1 x $10^5$ cells per well in a 24-well plate in 1 ml of cell culture medium (Table 9). *Salmonella* strains were grown overnight, subcultured the next day and grown for 3.5 h (2.1.1). After 3.5 h, 2 ml from the subculture were centrifuged at 6,000 x *g*, 2 min, RT and resuspended in 1.5 ml prewarmed PBS.

$OD_{600}$ was measured and adjusted to $OD_{600}$ of 0.2 which corresponds to approximately 3 x $10^8$ bacterial cells / ml (Geymeier 2011).

For the invasion assay HeLa cells were infected with a MOI of 20. The inoculum was prepared in 350 µl cell culture medium (Table 9) per well for each strain.

The culture medium from previously seeded HeLa cells was removed and 350 µl of the prepared inoculum were added to each well. For counting the bacterial cells in the inoculum, 350 µl were added to 650 µl prechilled PBS in a 1.5 ml tube. The plate was centrifuged at 300 x *g*, 5 min, RT to synchronise the infection and then incubated for 25 min at 37°C in the cell culture incubator, to allow *Salmonella* invasion of HeLa cells.

After incubation, medium was gently aspirated and cells were washed with 500 µl prewarmed PBS. The remaining extracellular bacteria were killed with 500 µl cell culture medium containing 100 µg/ml gentamicin. After 1 h in the cell culture incubator, the medium was removed and cells were washed three times with prewarmed PBS. HeLa cells were lysed with 500 µl of 0.5 % (v/v) sodium desoxycholate in PBS for 5 min at 37°C on a shaking platform. After vigorous pipetting, the lysate was transferred into a 1.5 ml tube with 500 µl prechilled PBS-T (PBS with 0.05 % (v/v) Tween 20). Serial dilutions were made with PBS-T for the samples and the inoculum. 100 µl from each dilution were plated on LB agar plates with respective antibiotics and incubated overnight at 37°C. Plates with CFU (colony forming units) between 30 - 300 were counted. Most suitable dilutions were for *S*. Typhimurium (WT): $10^{-3}$, *S*. Typhimurium with C26: $10^{-2}$, Δ*hilD* or Δ*invA* mutants: $10^0$ and ΔSPI4 mutants: $10^{-3}$. For the inoculum, the dilution $10^{-4}$ was plated twice.

### 2.5.4 Invasion assay of MDCK (NBL-2) cells

Protocol adapted from Gerlach et al. 2008; Wagner et al. 2011; Wagner et al. 2014.

MDCK (NBL-2) cells were seeded in a 24-well plate at a density of 1 x $10^5$ cells per well in 1 ml cell culture medium (Table 9) supplemented with 100 U $ml^{-1}$ penicillin and 100 µg $ml^{-1}$ streptomycin (Table 10) and grown for 5 – 6 days, to allow polarisation. The medium was changed every two days. One day prior to the experiment, the medium was changed to MEM without antibiotics (Table 9). After 5 days, approximately 18 x $10^5$ MDCK (NBL-2) cells were in each well.

*Salmonella* strains were grown overnight, subcultured the next day and grown for 3.5 h (2.1.1). After 3.5 h, $OD_{600}$ was measured and adjusted to $OD_{600}$ of 0.6 in PBS which corresponds to approximately 9 x $10^8$ bacterial cells per ml (Geymeier 2011). For the invasion assay of MDCK (NBL-2) cells, a MOI of 5 was used. The inoculum was prepared in 350 µl cell culture medium (Table 9) per well for each strain.

The culture medium was removed from MDCK cells and 350 µl of the inoculum were added to each well. Additionally, 350 µl of the inoculum were added to 650 µl prechilled PBS-T in a 1.5 ml tube to count the exact number of bacteria. The plate was centrifuged at 300 x *g*, 3 min, RT for synchronising the infection and then incubated for 25 min at 37°C in the cell culture incubator, to allow *Salmonella* invasion of MDCK cells. Subsequently, MDCK cells were washed three times with prewarmed PBS and 500 µl of cell culture medium (Table 9) with 100 µg/ml gentamicin were added to each well and incubated for 1 h in the cell culture incubator. MDCK cells were washed three times with prewarmed PBS and then lysed with 500 µl of 0.5 % (v/v) sodium desoxycholate in PBS for 15 min at 37°C on a shaking platform. After vigorous pipetting, the lysate was transferred into a 1.5 ml tube with 500 µl prechilled PBS-T (PBS with 0.05 % (v/v) Tween 20). Serial dilutions were plated on LB agar plates with respective antibiotics and incubated overnight at 37°C. All dilutions were plated and those with CFUs (colony forming units) between 30 - 300 were counted.

# 3 Results

## 3.1 C26 reduces SiiF expression and T1SS assembly

Aiming to assess the effect of the small molecule C26 on the expression of the SPI-4 *siiABCDEF* operon and on the assembly of the T1SS, the ABC-transporter protein SiiF was chromosomally labelled with a C-terminal 3xFLAG tag in different *Salmonella* strains: wild type (WT), Δ*hilD*, Δ*hilA* and Δ*invA*.
A Strep tag was also tested to label SiiF, but the fusion protein was not detectable on the immunoblot of the SDS-PAGE of whole cells (data not shown).

### 3.1.1 Effect of C26 on SiiF expression

To quantify the effect of C26 on SiiF expression, *Salmonella* strains were cultured in presence of increasing concentrations of C26 and cell lysates analysed by immunoblot (Figure 3).
In the Δ*invA* mutant, the deletion mutant of the major export apparatus protein of the T3SS-1, SiiF expression was similar to that of the WT which was expected as SPI-4 expression is, as far as we know, independent from InvA. No SiiF expression was observed in the negative controls Δ*hilD* and Δ*hilA* mutants (Figure 3).

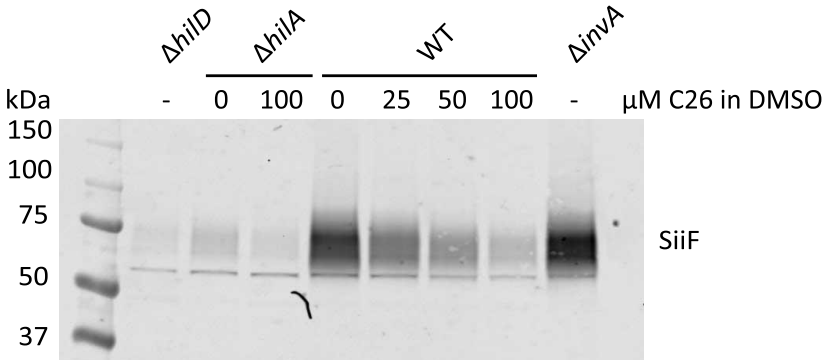


**Figure 3: Effect of C26 on SiiF-3xFLAG expression.**
Anti-FLAG immunoblot of SDS-PAGE from whole cells of *Salmonella* strains grown for 5 h in presence of different concentrations of C26 in 1 % DMSO or only 1 % DMSO, as indicated. Δ*hilD* and Δ*hilA* mutants are the negative control. WT (wild type).

A dose-dependent reduction of SiiF expression with increasing concentrations of C26 was observed in the wild type (WT). The addition of 100 µM C26 led to a reduction of SiiF expression similar to that of Δ*hilD* or Δ*hilA* mutant.

In the Δ*hilA* mutant slightly more SiiF was detectable compared to the Δ*hilD* mutant. The addition of 100 µM C26 further reduced SiiF expression in the Δ*hilA* mutant.

This experiment showed that at 100 µM, the small molecule C26 can reduce the expression of SiiF nearly to the same level as the Δ*hilD* mutant. Thus, it was assumed that C26 would also affect the assembly of the whole T1SS encoded on SPI-4.

### 3.1.2 C26 inhibits T1SS assembly

The effect of C26 on the T1SS assembly was assessed in the same mutant strains as those used for the quantification of SiiF expression level (Figure 3). As the SiiF mutations G500E and K506L inside the Walker box A of the nucleotide binding domain (NBD) abolish SiiF function (Gerlach et al. 2009), their effect on SiiF dimer formation and the assembly of the T1SS were also assessed (Figure 4c).

*Salmonella* WT and Δ*invA* mutant strains were treated with 25 µM and 100 µM C26 or 1 % DMSO as a control (Figure 4a, b). SiiF G500E and SiiF K506L mutants were grown without addition of C26 or DMSO (Figure 4c, d). Membrane protein complexes from the crude membranes fraction were analysed in native conditions and separated on the BN-PAGE (Figure 4a, c). In addition, membrane protein expression was further assessed on the SDS-PAGE (Figure 4b, d). In this case, the addition of the solubilisation buffer (SB) will disrupt solubilised membrane protein complexes.

Immunoblot of the corresponding BN-PAGE (Figure 4a) shows SiiF containing membrane protein complexes separated by their size. In the WT and Δ*invA*

mutant strain, a lower band at approximately 240 kDa and a higher band at approximately 900 kDa are visible. In presence of 100 µM C26, the upper band is absent and the lower band decreased to the same level as in the Δ*hilD* or Δ*hilA* mutant.

Compared to the WT strain, the Δ*invA* mutant showed an additional band with weak intensity above 1200 kDa, which disappeared at 100 µM C26.

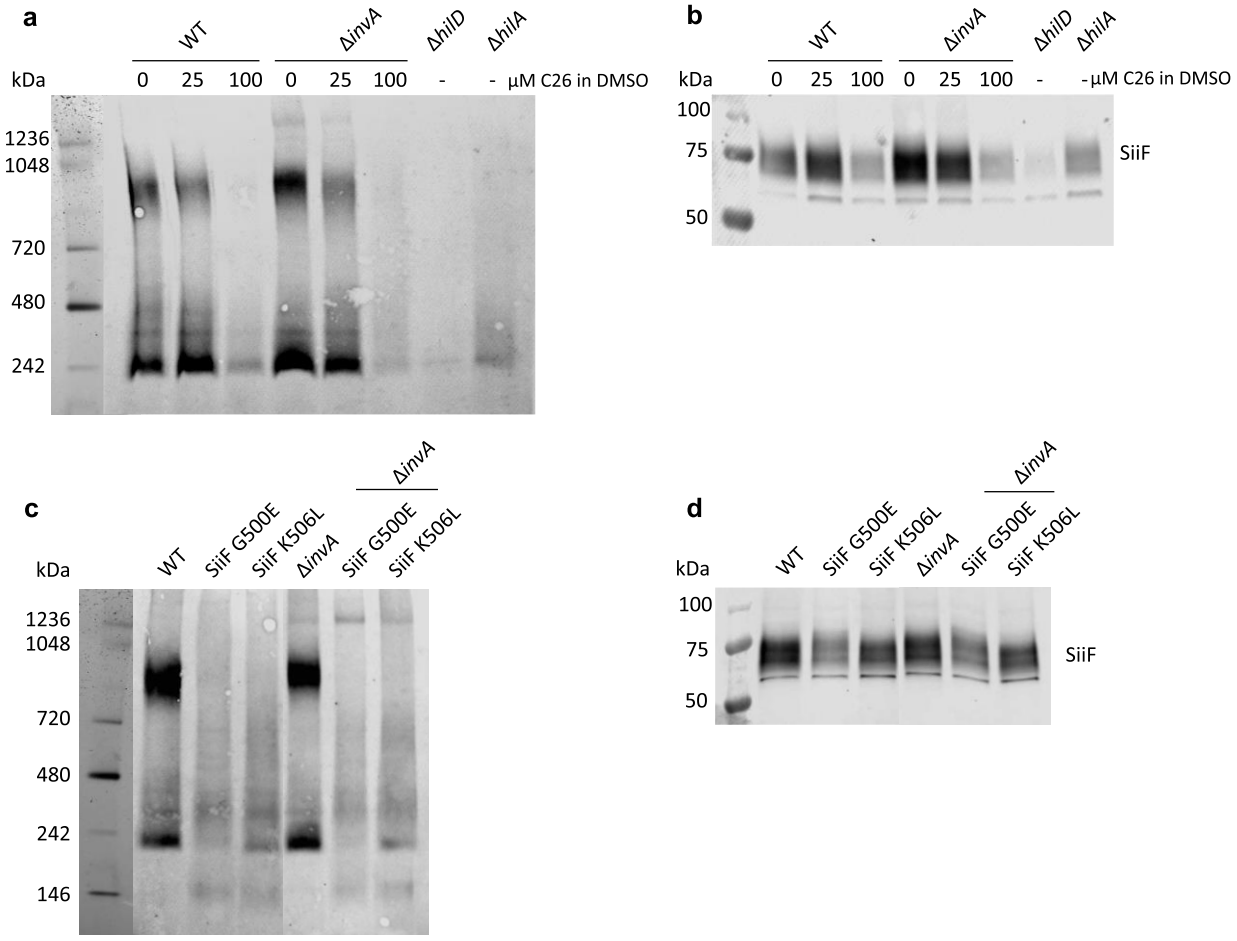


**Figure 4: Investigation of T1SS assembly and SiiF expression.**
Anti-FLAG immunoblots of BN-PAGE (a, c) and SDS-PAGE (b, d) from 6 ODU (optical density units) (a, b) and 8 ODU (c, d) crude membranes samples from SiiF-3xFLAG mutants. BN-PAGE (a, c) was used to separate solubilised membrane protein complexes. SDS-PAGE (b, d) was used to quantify SiiF protein expression level.
(a) BN-PAGE showing the effect of C26 on T1SS membrane protein complexes. Two complexes are visible that include SiiF, a lower band at 240 kDa and a higher band at 900 kDa. Increasing concentrations of C26 reduced assembly of both complexes in *Salmonella* wild type (WT) and Δ*invA* mutant strain.
(b) SDS-PAGE with a C26 dose dependent reduction of SiiF expression. Same samples as in (a) were used.
(c) BN-PAGE showing membrane protein complexes of SiiF G500E and K506L in the WT and Δ*invA* mutant background, respectively.
(d) SDS-PAGE from the same samples used in (c) to assess SiiF protein expression levels in SiiF mutant strains.

SDS-PAGE analysis revealed that treatment with 100 µM C26 reduced SiiF protein expression to a level comparable to the Δ*hilD* mutant (Figure 4b). This is in line with results obtained from the SDS-PAGE of whole cells (Figure 3).

The effect of SiiF G500E and SiiF K506L mutations on the T1SS assembly was investigated via BN-PAGE.
In BN-PAGE the 900 kDa membrane protein complex was not detected in the strains expressing the SiiF G500E and SiiF K506L variants (Figure 4c). In the SiiF G500E mutant, the 240 kDa band was very weak and a weak new band appeared at approximately 146 kDa. The same was observed for the SiiF K506L mutant, although the 240 kDa band was stronger compared to the SiiF G500E mutant.
Both variants were also expressed and analysed in the Δ*invA* mutant. A similar phenotype as that in the WT was observed. The Δ*invA* specific band at above 1200 kDa was visible in both mutants and apparently independent of SiiF membrane protein complexes.

Expression of SiiF harboring either of the mutations G500E and K506L was assessed on the SDS-PAGE (Figure 4d). While no difference in SiiF expression was found between WT and Δ*invA* strain, the SiiF protein harboring the mutation G500E proved to be more unstable than the wild type SiiF protein in both the WT and Δ*invA* strain.

Beside the effect of C26 on SiiF expression and T1SS assembly, a NanoLuc (Nluc) luciferase-based SiiE secretion assay was developed to assess the function of the SPI-4 encoded T1SS in response to C26.

## 3.2 Development of NanoLuc based SiiE secretion assay

Our lab has recently developed a NanoLuc luciferase-based secretion assay that allows quantification of protein secretion through T3SS-1 (Westerhausen et al. 2020). In this work, a Nluc based assay was developed for the quantification of full length SiiE secretion.

### 3.2.1 SiiE NanoLuc assay

To generate the SiiE::Nluc fusion protein, the Nluc enzyme was inserted at position K5411 of SiiE, between the 51 aa insertion and the BIg53 (Figure 5a). The aim of this assay was to assess the effect of C26 on SiiE secretion. Furthermore, the assay could be used to assess SiiE expression and surface retention. The luminescence signal from WT was set as 100 % and data were expressed as percentages of WT.

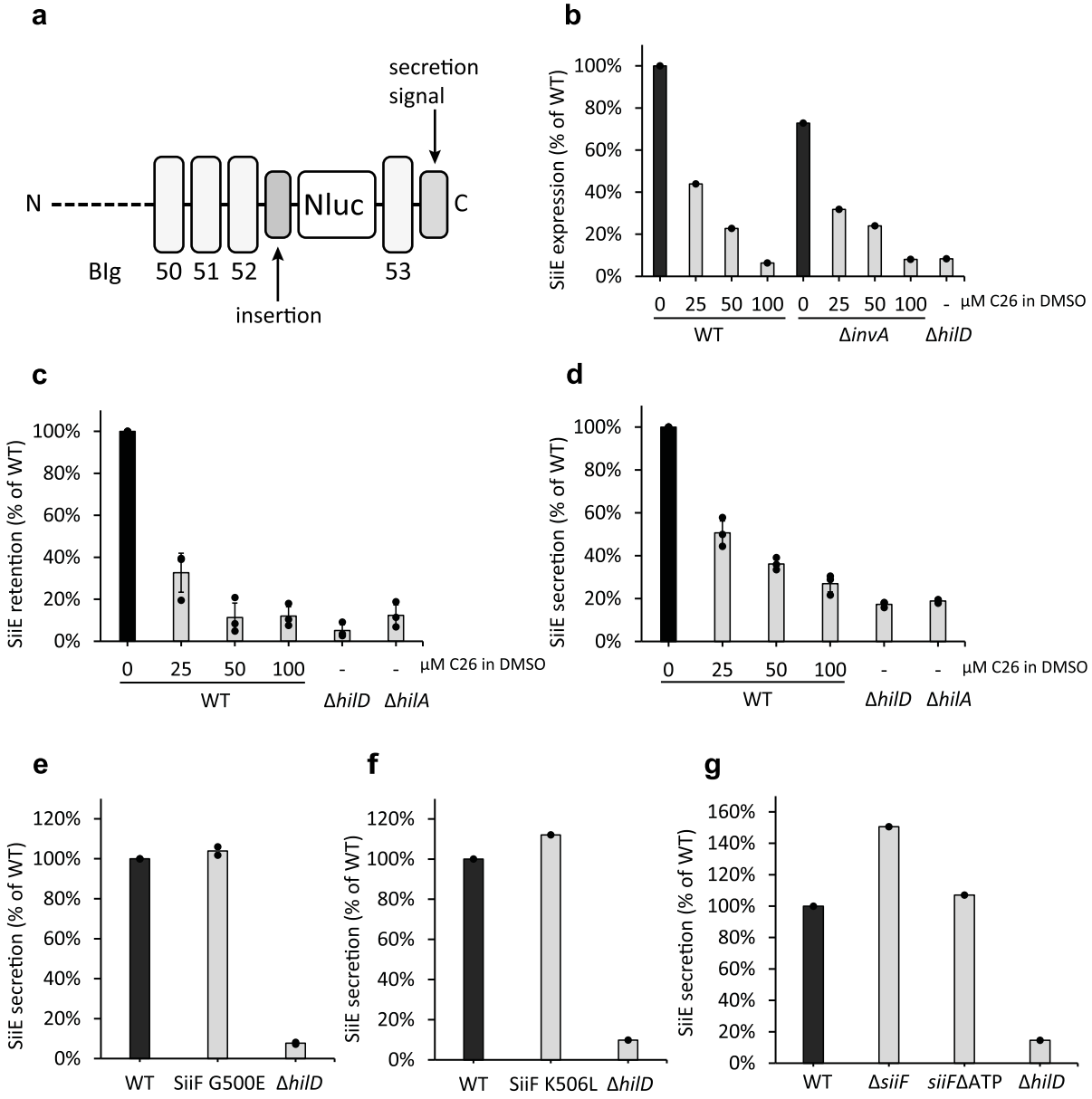


**Figure 5: SiiE NanoLuc assay.**
(a) Position of the inserted Nluc within the SiiE protein. Drawing of SiiE is not to scale. (b-d) Effect of C26 on SiiE expression (b), surface retention (c) and secretion (d).
(b) SiiE expression was quantified in 25 µl from the subculture using the Nano-Glo Live Cell Buffer and Substrate (ratio 1:50) system. Data shown are from one biological replicate.

(c-d) Effect of C26 on SiiE surface retention (c) and secretion (d). Bacterial cells were washed and resuspended in 250 µl PBS (c). HiBiT-Extracellular Buffer and Nano-Glo Extracellular NanoLuc Substrate (prototype) (ratio 1:50) was used to assess SiiE surface retention (c) and secretion (d). Data shown are means and standard deviations from three independent replicates.
(e-g) SiiE secretion in WT and different *siiF* mutants. The *siiF*ΔATP strain expresses a SiiF protein variant that lacks the ATP binding domain (SiiFΔN463-M688). Buffer Substrate mix was used like for (c, d). (e) Data shown are from two biological replicates and for (f, g) from one biological replicate. Luminescence signal for wild type (WT) was set as 100 % and data were expressed as percentages of WT (b-g). For (c), (d) and (e) means and standard deviations are shown. Black dots represent one replicate.

The effect of different concentrations of C26 on the expression of SiiE::Nluc fusion protein was assessed using the Nano-Glo LCS system (Table 8) and the results are shown in Figure 5b. SiiE expression was assessed in 25 µl of the subculture (bacterial cells and supernatant). There is a dose dependent reduction of SiiE expression for increasing concentrations of C26 in WT and Δ*invA* mutant strains (Figure 5b). At 100 µM, C26 reduced SiiE expression to the same level as the Δ*hilD* mutant. Interestingly, expression of SiiE was reduced in the Δ*invA* mutant to 72.8 % of the WT level.

In order to quantify the amount of SiiE bound to the outer cell envelope, a membrane impermeant NanoLuc substrate provided by Promega was used (prototype) (Table 8). Under the assumption that the used substrate is membrane impermeant and all SiiE from the supernatant was removed by washing steps, the observed luminescence signal from whole cell samples (bacterial cells) would correspond to SiiE expressed at the outer cell surface. C26 reduced SiiE surface fixation in a dose-dependent manner (Figure 5c). The Δ*hilD* and Δ*hilA* mutant strains were used as negative controls for SPI-4 gene expression. SiiE retention was reduced to 12 % of the WT level at concentrations of 100 µM C26, whereas in the Δ*hilD* and Δ*hilA* mutant strains SiiE retention was reduced to 5.1 % and 12.3 % of the WT level, respectively.

The culture supernatant was used to quantify SiiE secretion (Figure 5d). As observed for SiiE retention, the results show a dose-dependent reduction in SiiE secretion with increasing concentrations of C26. SiiE secretion was reduced to 27 % of the WT level at concentrations of 100 µM C26. In the Δ*hilD* and Δ*hilA* mutant strains SiiE secretion was reduced to 17.3 % and 18.9 % of the WT level, respectively.

Beside Δ*hilD* and Δ*hilA*, the mutant strains carrying the SiiF G500E and SiiF K506L variants were used as negative controls for SiiE secretion (Gerlach et al. 2009).

Surprisingly, SiiE was still secreted in both the SiiF G500E (Figure 5e) and SiiF K506L (Figure 5f) mutant strain. Similarly, secretion of SiiE was unexpectedly detected both, in a strain harbouring the SiiFΔN463-M688 mutant protein, which lacks the ATP binding domain (Table 4) and in the *siiF* null mutant strain (Δ*siiF*) (Figure 5g).

The results obtained from the SiiE::Nluc assay for the tested *siiF* mutants are inconsistent and the background signal in the Δ*hilD* and Δ*hilA* negative control strains is high. Thus, conclusions from the SiiE::Nluc assay should be interpreted with caution.

The 171 amino acid long NanoLuc enzyme was replaced by the 11 amino acid long HiBiT peptide.

### 3.2.2 SiiE HiBiT assay

The 33 bp long DNA fragment coding for HiBiT peptide was inserted into the *siiE* gene at amino acid position K5411, as illustrated in Figure 6a.

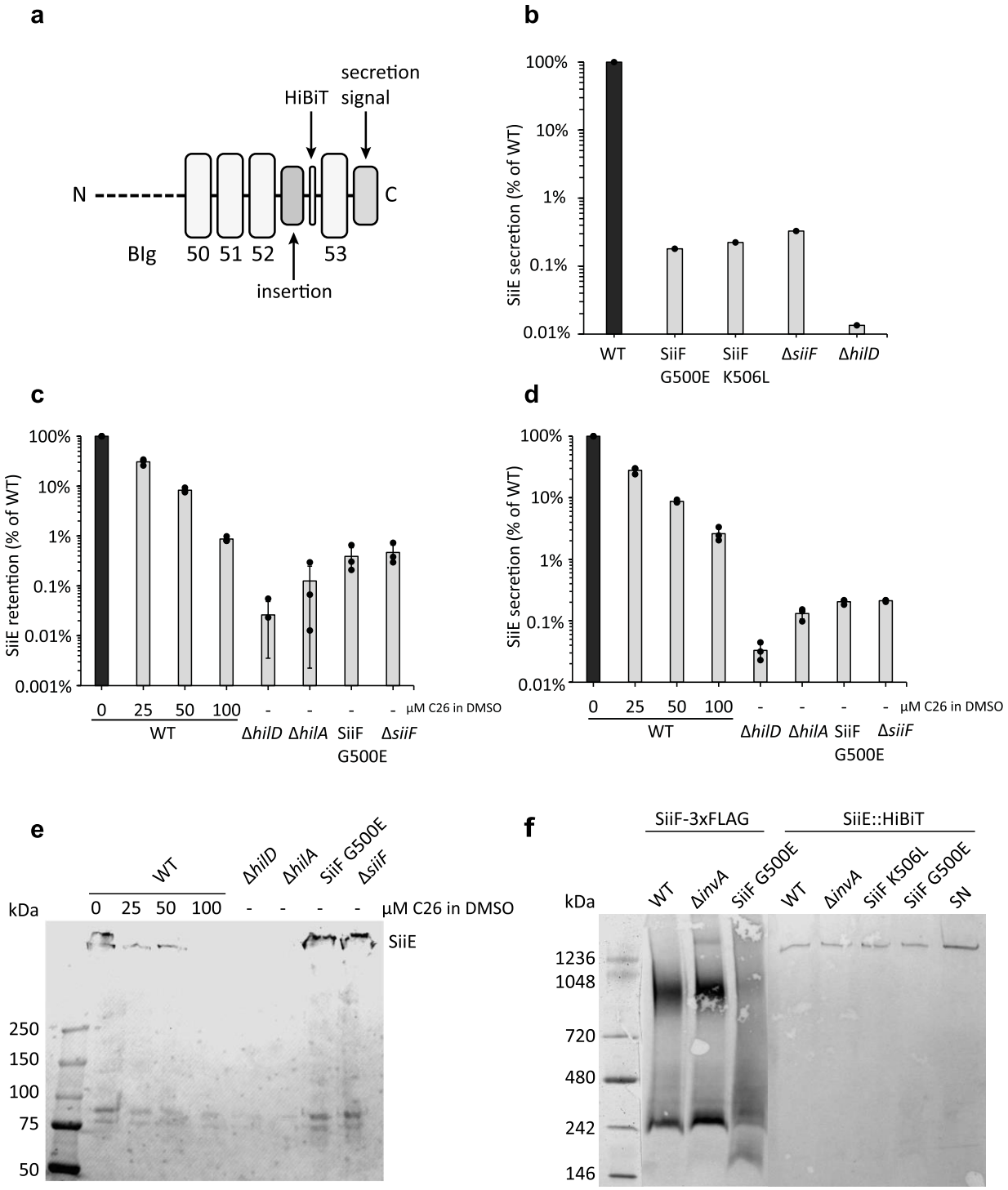


**Figure 6: SiiE HiBiT assay.**
(a) Position of the inserted HiBiT within the SiiE protein. Drawing of SiiE is not to scale.
(b) SiiE secretion in *Salmonella* wild type (WT) and different mutant strains. Luminescence was measured using Nano-Glo HiBiT Extracellular Buffer, Substrate (ratio 1:50) and LgBiT (ratio 1:100). Data shown are from one biological replicate.
(c-d) Effect of C26 on SiiE surface retention (c) and secretion into culture medium (d). Buffer, Substrate and LgBiT mix was used like for (b). Data shown are means and standard deviation from three independent replicates.
(e) C26 reduces SiiE expression. Anti-HiBiT immunoblot of SDS-PAGE from SiiE::HiBiT mutants. 0.5 ODU (optical density units) were harvested from one replicate used in (c, d). Whole cells were loaded on the 4 - 20 % SDS-PAGE and duration of electrophoresis was extended by 15 minutes.

(f) BN-PAGE of SiiF-3xFLAG and SiiE::HiBiT mutant strains. Crude membranes were prepared from 8 ODU cultures. Additionally, the concentrated supernatant (SN) of SiiE::HiBiT strain was loaded on the BN-PAGE. After Western Blotting, the membrane was cutted and the respective half of membrane was incubated with anti-FLAG or anti-HiBiT primary antibody. A merged image of both immunoblots is shown.

Secretion of SiiE::HiBiT was first tested in *Salmonella* WT, Δ*hilD* and different *siiF* mutants. As expected, SiiE was not secreted in the SiiF G500E, SiiF K506L and Δ*siiF* mutant strain (Figure 6b). In the Δ*hilD* negative control, SiiE secretion was reduced to 0.01 % of WT level.
Compared to the results from the SiiE::Nluc assay (Figure 5), these findings suggest that the SiiE::HiBiT assay is a more sensitive and reliable method to assess SiiE secretion.

Subsequently, SiiE::HiBiT assay was used to quantify the effect of C26 on SiiE retention at the bacterial cell surface (Figure 6c) and its secretion (Figure 6d).
It is assumed that the Nano-Glo HiBiT Extracellular Detection System (Table 8) measures only SiiE::HiBiT fusion proteins expressed at the cell surface or secreted into the supernatant. Treatment of *Salmonella* with 100 µM C26 reduced SiiE secretion to 2.6 % of the WT level (Figure 6d). However, in the Δ*hilD* and Δ*hilA* negative control, SiiE secretion was reduced to 0.03 % and 0.1 % of the WT level, respectively.
SiiE retention was reduced to 0.9 % of the WT level in presence of 100 µM C26 (Figure 6c). In the Δ*hilD* and Δ*hilA* mutant strains, SiiE retention was reduced similarly to what was observed for SiiE secretion.

The percentage of residual SiiE retention and secretion in the WT strain after C26 treatment was, however, higher than in the Δ*hilD* negative control (Figure 6c, d).
In order to assess SiiE protein production, 0.5 ODU of cultures were harvested from one of the three replicates used in the SiiE secretion assay (Figure 6c, d). Although the 595 kDa giant adhesin SiiE is too large for electrophoresis in a 4 - 20 % SDS-PAGE, immunodetection on the membrane after Western Blotting should be possible as SiiE should be located at the top of the gel. For this reason, electrophoresis time was prolonged by 15 minutes. On the corresponding anti-HiBiT immunoblot (Figure 6e) a band at the top of the gel is visible. It is

assumed that this band represents SiiE::HiBiT fusion protein. SiiE is not secreted in SiiF G500E and Δ*siiF* mutants (Figure 6d), but it is expressed and thus detectable in whole cells on the SDS-PAGE (Figure 6e). For WT strains treated with 100 µM C26 as well as Δ*hilD* and Δ*hilA* mutants, no SiiE is detectable on the anti-HiBiT immunoblot. The double band observed for the WT strain treated only with 1 % DMSO is most likely an artefact as the SDS-PAGE experimental conditions are not optimal for a large protein. These results suggest that C26 inhibits SiiE expression, whereas in the SiiF G500E and Δ*siiF* mutants only its secretion is impaired.

Since immunodetection of SiiE::HiBiT fusion protein was possible, the question arose whether SiiE could be present in the 900 kDa SiiF-containing membrane complex detected on the BN-PAGE (Figure 4a).
Beside crude membranes samples, 2 ml of concentrated supernatant (SN) from the SiiE::HiBiT mutant was loaded on the BN-PAGE (Figure 6f). In the SiiF-3xFLAG mutants the same membrane complexes are detectable as described in Figure 4a. A band with weak intensity above 1200 kDa is detectable for all SiiE::HiBiT crude membrane samples. The same band is detectable in the sample from supernatant (SN). Hence, it can be concluded that SiiE is not present in the 900 kDa complex observed in SiiF-3xFLAG mutants.

So far, the effect of C26 was shown on SiiE secretion in an end-point measurement after 5 h of growth. The established SiiE::HiBiT assay was used to follow SiiE secretion overtime.

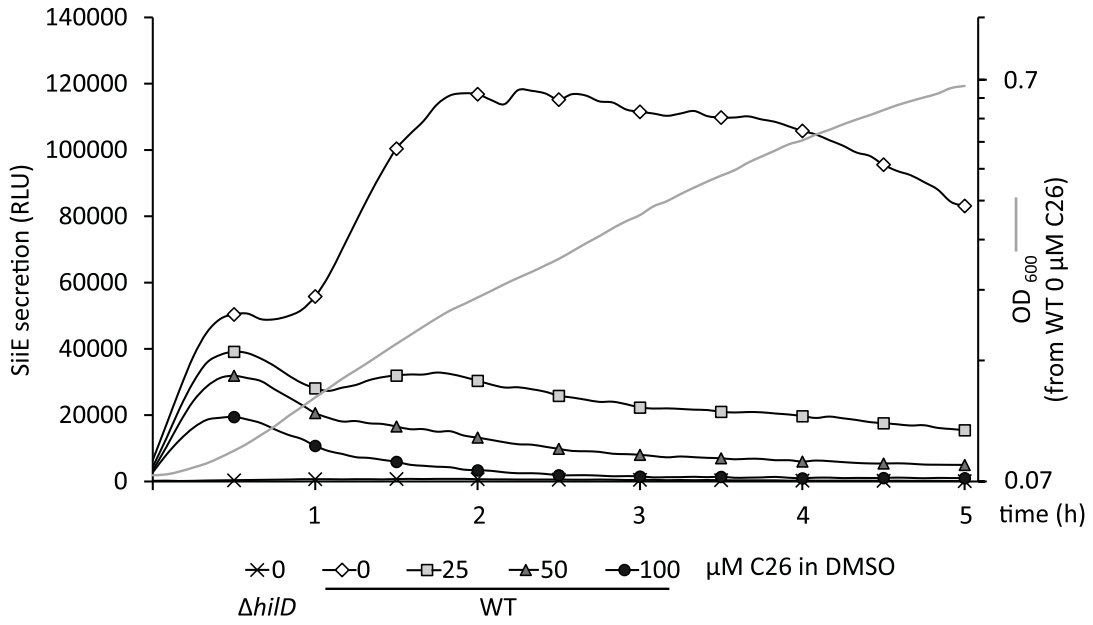


**Figure 7: SiiE secretion kinetic.**
*Salmonella* wild type (WT) and Δ*hilD* mutant strains were grown overnight. Bacterial cells were washed twice in PBS before subculturing. Strains were subcultured in a volume of 125 µl composed of 100 µl prewarmed LB 0.3 M NaCl and 25 µl of Nano-Glo HiBiT Extracellular Buffer, Substrate (ratio 1:50) and LgBiT (ratio 1:100) to an $OD_{600}$ of 0.1 in a 96-well plate. Different concentrations of C26 in 1 % DMSO were added to the wells as indicated. The 96-well plate was placed in a humidity cassette in the 37°C prewarmed Tecan plate reader. Relative light units (RLU) and $OD_{600}$ was measured every 5 min for 5 hours. Data shown are from one replicate.

Therefore, *Salmonella* strains were subcultured in a 96-well plate in a Tecan plate reader. Different growth conditions and mixes of Nano-Glo HiBiT Buffer Substrate LgBiT were tested, until optimal conditions were found. Strains were subcultured to an $OD_{600}$ of 0.1 in 125 µl medium composed of 100 µl prewarmed LB 0.3 M NaCl and 25 µl of the Nano-Glo HiBiT Extracellular Buffer, Substrate (ratio 1:50) and LgBiT (ratio 1:100) master mix. In order to remove all SiiE already secreted into the supernatant overnight, bacterial cells were gently washed twice in prewarmed PBS.

The assay was performed in replicates, but different behaviours according to bacterial growth and maximal SiiE secretion were observed (Figure 7).
SiiE secretion reached its maximum after 120 min of growth, corresponding to mid-exponential growth phase. After 180 min, SiiE secretion decreased. In presence of different concentrations of C26, SiiE secretion was reduced. Within

the first 30 min, a clear reduction of SiiE secretion is seen for 100 µM C26 (Figure 7).

In summary, the data represented so far indicate that C26 inhibits SiiF expression, T1SS assembly (3.1) and SiiE secretion (3.2.2).

In the last part of this work, the activity of C26 and the role of SPI-4 in T3SS-1 mediated *Salmonella* pathogenicity were investigated.

## 3.3 Effect of C26 on host cell invasion

In light of the inhibitory activity of C26 on SiiF expression (Figure 3), T1SS assembly (Figure 4a) and SiiE secretion (Figure 6d), we speculated that C26 would negatively impact adhesion to and subsequently invasion of polarised epithelial cells, a hypothesis that I set out to investigate here.

First, culture conditions were optimised for the invasion assay in light of reports that SiiE is retained only temporarily on the bacterial surface and SiiE surface expression decreases overtime (Wagner et al. 2011). Therefore, to ensure that *Salmonella* expressed SiiE (SPI-4) and SipA (SPI-1) when exposed to (non-polarised) HeLa and (polarised) MDCK cells, SipA-HiBiT and SiiE::HiBiT secretion into culture medium were quantified overtime (Figure 8).

More specifically, *Salmonella* strains were subcultured for 5.5 h and secretion of SiiE::HiBiT and SipA-HiBiT was assessed at different times. For each measurement (Figure 8), an independent subculture was used to avoid effects on bacterial growth and gene expression through changes in volume, temperature or aeration. Additionally, $OD_{600}$ was measured to follow bacterial growth.

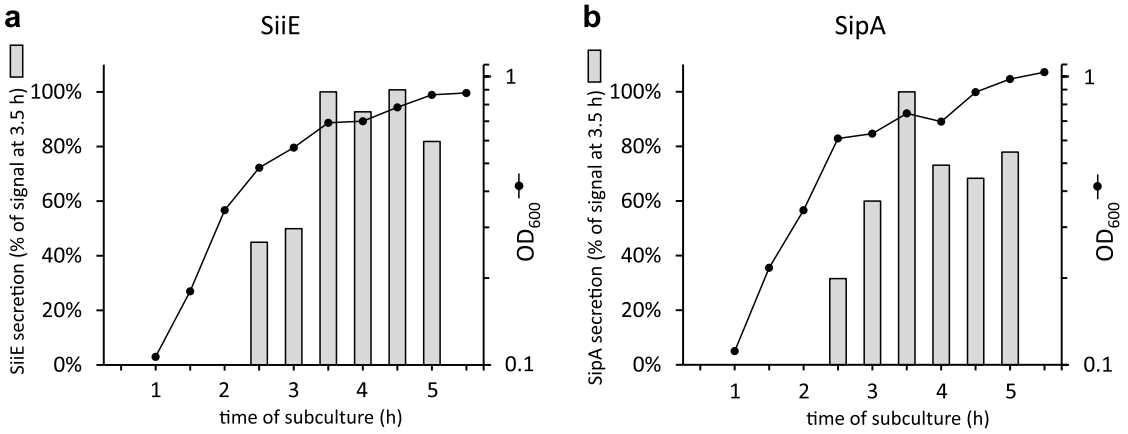


**Figure 8: Quantification of SiiE and SipA secretion overtime.**
*Salmonella* SiiE::HiBiT (a) and SipA-HiBiT (b) mutant strains were subcultured and at the indicated times SiiE and SipA secretion and $OD_{600}$ were measured. For each measurement, an independent subculture was used. Secretion into culture medium was measured from 2.5 - 5 h of subculture as indicated. Luminescence was measured using Nano-Glo HiBiT Extracellular Buffer, Substrate (ratio 1:50) and LgBiT (ratio 1:100). Data shown are from individual subcultures of one biological replicate. SiiE::HiBiT and SipA-HiBiT secretion signal after 3.5 h of subculture were set as 100 %. Figure design adapted from Wagner et al. 2011.

Results show that SiiE (Figure 8a) and SipA (Figure 8b) secretion peaks at 3.5 h when bacteria are in the late exponential growth phase. The amount of SiiE and SipA secreted in the culture medium were slightly reduced after 5 h of growth compared to 3.5 h.

In conclusion, 3.5 h of subculture ensures SipA (SPI-1) and SiiE (SPI-4) expression and secretion, which should allow adhesion to polarised cells and subsequent host cell invasion. This growth time was used for the following invasion (Figure 9) and SipA-HiBiT injection assay (3.4).

The gentamicin protected invasion assay was used to quantify *Salmonella* invasion of HeLa and MDCK (NBL-2) cells. Invaded bacteria were expressed as percentages of the inoculum.

First, invasion of non-polarised HeLa cells was assessed (Figure 9a). For the WT strain, approximately 11.7 % of the bacteria from the inoculum invaded HeLa cells. The ΔSPI4 mutant behaved similarly to the WT strain with approximately 13.6 % of the bacteria invading HeLa cells. In the Δ*hilD* and Δ*invA* negative control strains invasion of HeLa cells was reduced to approximately 0.03 % of the bacteria from the inoculum.

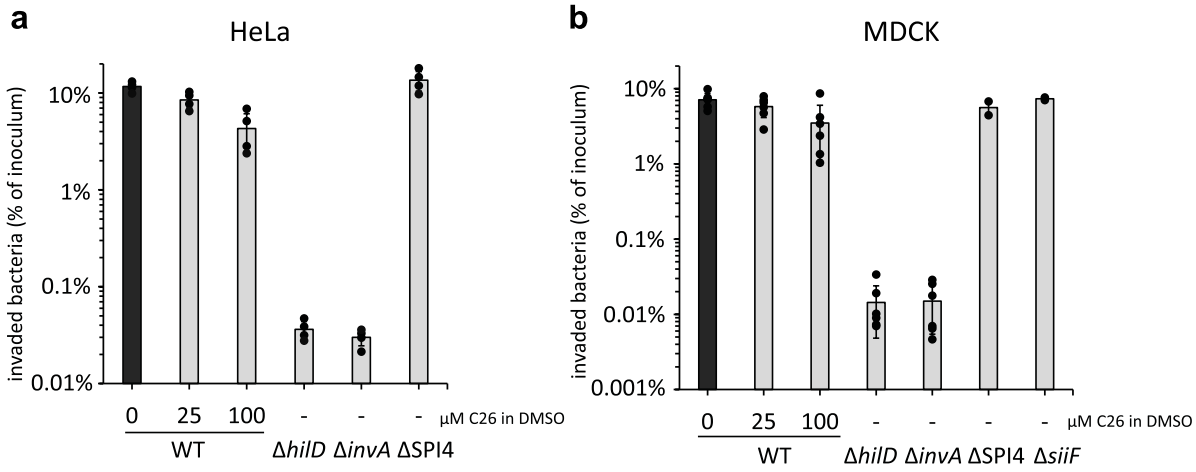


**Figure 9: *Salmonella* invasion of HeLa and MDCK cells.**
(a) HeLa cells were infected at a MOI of 20 and (b) MDCK cells were infected at a MOI of 5 for 25 minutes. Infection was synchronised by centrifugation step. *Salmonella* strains were grown for 3.5 h in presence of C26. After 25 min, infected cells were washed and gentamicin was added to the medium to remove all extracellular and adherent bacteria. Intracellular bacteria and bacteria in the initial inoculum were counted after plating onto agar plates. Data shown are means and standard deviations of intracellular bacterial numbers expressed as percentages of the numbers in the initial inoculum. Invasion assay for HeLa cells (a) was performed in four independent replicates and MDCK cell invasion assay (b) in six independent replicates. ΔSPI4 and Δ*siiF* mutants were used only in two replicates of MDCK cell invasion assays (b). Data shown are means with standard deviation. Each dot represents one replicate.

*Salmonella* grown in presence of C26 was attenuated in HeLa cell invasion (Figure 9a). Culturing bacteria in 25 µM or 100 µM C26 reduced invasion of HeLa cells to 8.5 % and 4.3 % of the bacteria from the inoculum, respectively. Hence, *Salmonella* treated with 100 µM C26 displayed a level of HeLa cell invasion equal to 36.9 % of the untreated wild type level (Figure 9a).

Second, invasion of MDCK (NBL-2) cells was investigated (Figure 9b). MDCK cells were allowed to grow for 5 - 6 days in order to get a polarised cell monolayer (2.5.4).

For the WT strain, approximately 7.1 % of the bacteria from the inoculum invaded MDCK cells. Contrary to expectations, the invasion capacity of the ΔSPI4 and Δ*siiF* mutants into MDCK cells was not strongly reduced. In the ΔSPI4 and Δ*siiF* mutant strain, approximately 5.6 % and 7.4 % of the bacteria from the inoculum invaded MDCK cells, respectively. According to these results it can be assumed that MDCK cells used in this study were most likely not properly polarised.

In the Δ*hilD* and Δ*invA* negative control strain invasion of MDCK cells was reduced to approximately 0.015 % of the bacteria from the inoculum. The deletion

of SPI-4 or *siiF* was expected to have a similar effect as observed for the SPI-1 deficient Δ*invA* mutant strain.
The addition of 25 µM and 100 µM C26 to the growing bacteria reduced invasion of MDCK cells to approximately 5.8 % and 3.5 % of the bacteria from the inoculum, respectively. Hence, treatment with 100 µM C26 reduced *Salmonella* invasion of MDCK cells to a level equal to 49.2 % of the untreated wild type level (Figure 9b).

In conclusion, invasion of non-polarised HeLa cells was reduced to 36.9 % and invasion of most likely non-polarised MDCK cells was reduced to 49.2 % of the WT level in presence of 100 µM C26.

## 3.4 Effect of C26 and role of SPI-4 for T3SS-1 injection

As shown above (Figure 9) SPI-4 was not required for invasion of HeLa cells and unfortunately also not required for invasion of the MDCK cells used in this study. It can be hypothesised that T3SS-1 mediated injection of effector proteins into HeLa cells should occur independently of SPI-4.

In order to assess the role of SPI-4 and the effect of C26 on T3SS-1 injection of effector proteins into HeLa-LgBiT cells, a split luciferase (HiBiT-LgBiT) assay developed in our lab was used (Westerhausen et al. 2020). This assay allows quantification of the injection of T3SS-1 effector proteins fused to HiBiT into HeLa cells stably expressing LgBiT (HeLa-LgBiT). Briefly, HeLa-LgBiT cells were infected with *Salmonella* strains expressing SipA-HiBiT. After injection of SipA-HiBiT into HeLa-LgBiT, HiBiT and LgBiT reconstitute the luciferase and addition of a Nano-Glo Live Cell Substrate will result in a luminescence signal. Luminescence was measured every 5 min in a kinetic measurement for 3 hours.

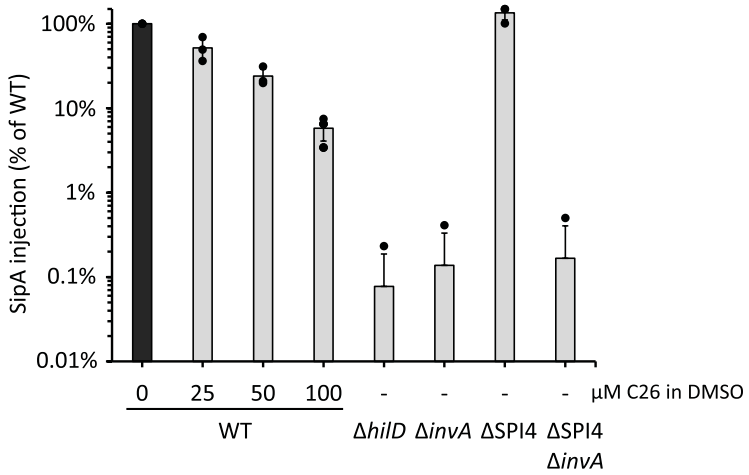


**Figure 10: SipA-HiBiT injection into HeLa-LgBiT cells.**
SipA-HiBiT injection was compared between *Salmonella* wild type (WT) strains treated with increasing concentrations of C26 and different mutant strains. HeLa-LgBiT cells were infected with different *Salmonella* strains (MOI 50). At time zero of infection, Nano-Glo Live Cell Buffer and Substrate (ratio 1:20) was added to the infected cells. Data shown are from the luminescence measurement 120 min after infection. WT signal was set as 100 % and data were expressed as percentages of WT. Data shown are means with standard deviations of three independent assays. Each dot represents one independent assay that was performed with 3 technical replicates.

SipA-HiBiT injection was similar for WT and ΔSPI4 mutant strain, indicating that SPI-4 is not required for injection of SipA-HiBiT into HeLa-LgBiT cells (Figure 10). Interestingly, in the ΔSPI4 mutant, SipA-HiBiT injection was increased to 135 % of the WT signal.

Addition of C26 reduced SipA-HiBiT injection in a dose-dependent manner (Figure 10). At 100 µM C26, SipA-HiBiT injection was reduced to 5.8 % of the WT signal. However, in the Δ*hilD* and Δ*invA* negative control strains injected SipA-HiBiT was reduced to approximately 0.08 % and 0.14 % of the WT signal, respectively. The ΔSPI-4 Δ*invA* mutant behaved similarly to the Δ*invA* mutant.
In conclusion, SPI-4 did not contribute to T3SS-1 SipA-HiBiT injection into non-polarised HeLa-LgBiT cells and 100 µM C26 reduced SipA-HiBiT injection to 5.8 % of the WT signal.

A similar approach should have been used to investigate the role of SPI-4 in T3SS-1 effector protein injection into polarised cell monolayers. However, this required the generation of polarised cell lines, like MDCK or CaCo-2, that stably expressed LgBiT. Towards this goal, a preliminary experiment to transiently

transfect MDCK cells with a plasmid containing LgBiT was performed (data not shown). Due to time constraints the establishment of this cell line was not achieved. Additionally, optimal cell culture conditions for the generation of a polarised epithelial cell monolayer have to be established first.

# 4 Discussion

## 4.1 C26 reduces SiiF expression

The aim of the first part of this work was to investigate the effect of C26 on SPI-4 gene expression. Therefore, expression of SiiF-3xFLAG fusion protein in presence of different concentrations of C26 was assessed. A dose dependent reduction in SiiF expression in *Salmonella* WT strains treated with 25 µM, 50 µM or 100 µM C26 was observed (Figure 3). It is important to note that in presence of 100 µM C26, SiiF expression is reduced to nearly the same level as that of the negative controls Δ*hilD* or Δ*hilA*. In the same way, SiiE::HiBiT expression was reduced as evidenced by SDS-PAGE analysis of whole cell samples (Figure 6e).

In this study, conclusion can be drawn only for SiiF (Figure 3) and SiiE (Figure 6e) expression. However, the six genes *siiABCDEF* on SPI-4 presumably form one 24 kb long transcriptional unit, with a transcriptional start site located upstream of *siiA* (Figure 1a) (Gerlach et al. 2007a; Main-Hester et al. 2008). It must be noted that a second independent transcriptional start site located 128 bp upstream of *siiF* was previously speculated (Main-Hester et al. 2008).
Still, the observed reduction in SiiF (Figure 3) and SiiE (Figure 6d) expression is most likely representative of the whole *sii* operon. This would be in line with the observed reduction of SiiF containing membrane protein complexes in presence of C26 (Figure 4a).

Although HilA is described as the transcriptional activator of SPI-4 (Ahmer et al. 1999; Gerlach et al. 2007a; Morgan et al. 2007; Main-Hester et al. 2008) by binding near to the promotor region of the *sii* operon (Thijs et al. 2007; Main-Hester et al. 2008), the Δ*hilA* mutant showed slightly more SiiF expression compared to the Δ*hilD* mutant (Figure 3). The difference is even clearer on the SDS-PAGE after crude membranes preparation (Figure 4b).
Small variations of the band intensity on the immunoblot should be treated with considerable caution because no protein loading control was used. A source of

error can occur in the whole row of sample preparation and sample loading. Nevertheless, this can be interpreted as a sign that, to a small extent, SiiF expression occurs independently from HilA.
The effect of C26 on SiiF expression was also tested in a Δ*hilA* mutant. It was observed that 100 µM C26 can further reduce SiiF expression, albeit slightly (Figure 3). Is SiiF or more generally SPI-4 expressed to a small extent in a HilD dependent, but HilA independent manner?

Gerlach et al. used a luciferase-based assay to investigate the expression level of SPI-4 fusion proteins in different background mutant strains. In a *sirA* deficient mutant, *siiA*::luc expression was reduced 96-fold. Intriguingly, in the *hilA* deficient mutant *siiA*::luc, *siiE*::luc and *siiF*::luc expression were only 6.3-, 8.6- and 7.3-fold reduced, respectively (Gerlach et al. 2007a). In line with this, the ELISA assay revealed that SiiE secretion was less attenuated in the *hilA* mutant compared to the *sirA* mutant (Geymeier 2011).
Main-Hester et al. assessed the transcription level of *siiE* via qRT-PCR and found higher expression levels in the *hilA* mutant than in the *sirA* mutant (Main-Hester et al. 2008).
These results seem to suggest that SirA activates SPI-4 expression also in a HilA independent way (Gerlach et al. 2007a; Main-Hester et al. 2008; Geymeier 2011). Petrone et al. reported that *siiA* is directly regulated through HilD, HilC, RtsA and HilA (Petrone et al. 2014), which activate *siiA* transcription most likely by counter silencing the repressing effect of H-NS (Smith et al. 2016). A similar mechanism was described for HilA, which antagonises H-NS and thus activates SPI-4 expression (Main-Hester et al. 2008).

To summarise, I was able to show that 100 µM C26 strongly reduces SiiF-3xFLAG expression (Figure 3). It can further be speculated that SiiF may be expressed to a small extent independently from HilA, which is in line with previous findings (Gerlach et al. 2007a; Main-Hester et al. 2008; Geymeier 2011; Petrone et al. 2014). However, further work is required to elucidate the regulation of SPI-4 expression.

## 4.2 C26 inhibits T1SS assembly

Beside assessing the effect of C26 on SiiF expression, the effect on the assembly of the T1SS was investigated.

SiiF-3xFLAG containing membrane protein complexes were detected in two major bands at approximately 240 kDa and 900 kDa on the BN-PAGE (Figure 4a). There is a clear dose-dependent reduction of the SiiF containing membrane protein complexes in both the WT and Δ*invA* strains treated with 25 µM and 100 µM C26.

At 100 µM C26 the 900 kDa membrane protein complex disappeared and the protein complex at 240 kDa was reduced to nearly the same level as in the Δ*hilD* mutant (Figure 4a). There is only a small difference between the Δ*hilD* and Δ*hilA* mutant regarding the intensity of the 240 kDa band. This suggests that SiiF containing membrane protein complexes are only slightly expressed independently from HilA. The small difference can also be due to variations in the amount of loaded proteins per sample.

Interestingly, there is an additional weak band above 1200 kDa for all Δ*invA* mutant strains on the BN-PAGE (Figure 4 a,c). So far, it is not known why this band appears only in the Δ*invA* mutant strain but not in the WT.

The most important limitation of this experiment is that only SiiF-3xFLAG can be detected on the immunoblot. Thus, only speculations can be drawn with respect to the other proteins that are present within the membrane in complex with SiiF. Several combinations are possible and they are discussed briefly below.

The T1SS encoded on SPI-4 is predicted to consist of the ABC-transporter SiiF, the MFP SiiD and the OMP SiiC (Morgan et al. 2004; Gerlach et al. 2007b; Main-Hester et al. 2008). SiiA and SiiB are supposed to form a proton channel in the inner membrane and SiiB was shown to interact with SiiF (Wille et al. 2014). Wille et al. suggested a stoichiometry of 2:4 for SiiA and SiiB (Wille et al. 2014).

Based on the stoichiometry of the HlyA T1SS in *E. coli* (Kanonenberg et al. 2018; Spitz et al. 2019), it can be hypothesised that the OMP SiiC is a trimer, the MFP SiiD a trimer or a hexamer and the ABC-transporter SiiF a dimer. This would

result in SiiCDF (3:6:2) membrane protein complex of a size of 564 kDa. Solubilised in LMNG, the micelle of the complex could run at 900 kDa on the BN-PAGE (Figure 4a) (Samuel Wagner, personal communication 2021).
In the HlyA T1SS the OMP TolC is recruited to the HlyB-HlyD (ABC-transporter-MFP) complex only in presence of the substrate HlyA (Spitz et al. 2019). It was already suggested that this could also be the case for the T1SS encoded on SPI-4 (Wille et al. 2014).

The ABC-transporter protein SiiF is sized at approximately 75 kDa. It is possible that the micelle of the LMNG solubilised SiiF dimer runs at 240 kDa on the BN-PAGE (Figure 4a). The membrane protein complex at 240 kDa or at 900 kDa could also include SiiB or the previously described SiiA and SiiB inner membrane protein complex (Wagner 2011; Wille et al. 2014; Kirchweger et al. 2019).

Wille et al. reported that the point mutation G500E in the Walker A motif of the nucleotide-binding domain (NBD) of the ABC-transporter SiiF prevents SiiF dimer formation, which is most likely dependent on the integrity of the NBD (Wille et al. 2014). Therefore, the SiiF G500E and SiiF K506L mutants (Gerlach et al. 2009) were used to investigate the effect of both point mutations on the T1SS membrane protein complexes visible on the BN-PAGE (Figure 4c). The 900 kDa band was absent in both mutants and the 240 kDa band was strongly reduced (Figure 4c). It can be assumed that mutations inhibiting SiiF dimer formation further prevent the assembly of the whole T1SS. If the 240 kDa band consists of LMNG solubilised SiiF dimers, the results presented here are in line with the observation made by Wille et al. through B2H and FRET and confirm that the SiiF G500E mutation prevents SiiF dimer formation (Wille et al. 2014).

In the SiiF K506L mutant the 240 kDa band is stronger compared to SiiF G500E (Figure 4c). This would suggest that the SiiF K506L variant to some extent still forms dimers. Wille et al. did not analyse the effect of the K506L mutation on SiiF dimer formation, which would be interesting to investigate by B2H and FRET (Wille et al. 2014).

Interestingly, a new weak band at 146 kDa appeared on the BN-PAGE for both mutants that was not present in the WT (Figure 4c). It could be possible that the 146 kDa band represents LMNG solubilised SiiF proteins.

It was further reported that the G500E mutation reduces SiiF expression (Wille et al. 2014). Although no protein loading control was used, the results from the SDS-PAGE (Figure 4d) confirm that SiiF expression is reduced in the SiiF G500E mutant as compared to the level in WT or Δ*invA* mutant. In contrast, only a small reduction is seen for the SiiF K506L mutant.
The reason for reduced expression in SiiF G500E and the difference between the SiiF G500E and K506L mutation has yet to be determined.

In conclusion, 100 µM C26 reduced SiiF expression and prevented assembly of the T1SS to a level similar to the Δ*hilD* or Δ*hilA* mutant. However, further work is required to solve the stoichiometry and structure of the T1SS encoded on SPI-4, especially with regard to the inner membrane proteins SiiA and SiiB as novel T1SS subunits (Wagner 2011; Wille et al. 2014; Kirchweger et al. 2019).

## 4.3 SiiE secretion assay

The aim of this part of the project was to establish a NanoLuc (Nluc) luciferase-based SiiE secretion assay. An ELISA (Morgan et al. 2007; Geymeier 2011) and a *Gaussia princeps* luciferase (Gluc) based assay (Wille et al. 2012; Peters et al. 2017) have already been established and can be used to assess secretion of chromosomally or episomally expressed SiiE, respectively. Where to insert NanoLuc to generate a SiiE::Nluc fusion protein was a decision to be made.

Wille et al. tested different Gluc::SiiE proteins, where Gluc was fused to the N-terminus of C-terminal SiiE fragments (Wille et al. 2012). Gluc fusion to the N-terminus of a BIg50-53 SiiE fragment was secreted efficiently into the supernatant (Wille et al. 2012). When Gluc was fused to the N-terminus of a BIg53 fragment, it led to a reduced secretion of only 5 % of the BIg50-53 fusion protein level (Wille et al. 2012).

Wagner et al. assessed the requirement for secretion of chromosomally expressed SiiE by ELISA. Without the BIg53 domain and the C-terminal secretion signal, SiiE is not secreted (Wagner et al. 2011). Interestingly, deletions of BIg52 or the 51 aa insertion between BIg52 and BIg53 (Figure 1b) do not affect SiiE secretion, surface retention or invasion of polarised cells (Wagner et al. 2011).

The 513 bp long NanoLuc luciferase was inserted upstream of BIg53 at amino acid position K5411 (Figure 5a). In analogy to the Gluc fusion protein, Nluc could have also been inserted upstream of BIg50 (Wille et al. 2012).
However, in contrast to the established Gluc assay, Nluc was fused into the chromosome of SiiE. Beside secretion into the supernatant, this method could also be used to quantify the amount of SiiE retained on the bacterial cell surface, in analogy to an ELISA, epifluorescence microscopy or dot blots analysis (Wagner et al. 2011).
Initially, the results of the SiiE::Nluc assay were intuitive as C26 reduced SiiE expression (Figure 5b) for WT and Δ*invA* mutants in a dose-dependent manner. Interestingly, SiiE expression was reduced in the Δ*invA* mutant strain compared to the WT level (Figure 5b). A similar observation was previously made by Main-Hester et al. who reported reduced SiiE secretion in a SPI-1 deficient Δ*invA* mutant strain (Main-Hester et al. 2008). Further work is required to elucidate why SiiE expression (Figure 5b) and secretion (Main-Hester et al. 2008) are reduced in a Δ*invA* mutant.

The SiiE::Nluc assay was used to quantify SiiE retention and secretion using the Extracellular NanoLuc Substrate (Promega, prototype) (Table 8). Although C26 reduced SiiE retention and secretion in a dose-dependent manner, there was a high background level in the Δ*hilD* and Δ*hilA* negative control strains (Figure 5c, d). Additionally, results suggest that SiiE was still secreted in all four tested *siiF* mutant strains (Figure 5e-g), where other authors have shown that SiiE is not secreted (Gerlach et al. 2007b; Kiss et al. 2007; Morgan et al. 2007; Main-Hester et al. 2008; Gerlach et al. 2009).

Thus, results from the SiiE::Nluc assay must be discussed critically. It is not known, which effect the insertion of the 512 bp long NanoLuc enzyme exerts on SiiE expression, structure or secretion. It is also not known whether full length SiiE is expressed and secreted, nor whether secretion occurs through the T1SS at all. SiiE::Nluc fusion protein was also not detectable in a supernatant sample on the BN-PAGE or SDS-PAGE with respective antibodies (data not shown).
To summarise, the results obtained from the SiiE::Nluc secretion assay should be interpreted with considerable caution, as they are not in line with previous findings regarding non-secreting *siiF* mutants (Gerlach et al. 2007b; Kiss et al. 2007; Morgan et al. 2007; Main-Hester et al. 2008; Gerlach et al. 2009). Insertion of NanoLuc at this position is most likely not suitable for quantifying SiiE secretion.

In a second approach, NanoLuc was replaced by the 33 bp long HiBiT fragment (Figure 6a). It is assumed that the 11 aa long HiBiT peptide can be well accommodated and would have a minor, if any, effect on the protein function (Lee 2017; Westerhausen et al. 2020). HiBiT could also have been inserted upstream of BIg50, in analogy to the Gluc::SiiE fusion protein (Wille et al. 2012). Of note is that the Nano-Glo HiBiT Extracellular Detection System (Table 8) only detects extracellular SiiE::HiBiT fusion proteins, because the larger subunit LgBiT cannot enter the bacterial membrane (Samuel Wagner, personal communication 2021).

SiiE secretion was reduced in all tested SiiF mutant strains (Figure 6b), which is in line with previous findings (Gerlach et al. 2007b; Kiss et al. 2007; Morgan et al. 2007; Main-Hester et al. 2008).
In the SiiE::HiBiT assay SiiE secretion was reduced to 0.03 % of the WT level in the Δ*hilD* negative control (Figure 6d), whereas in the SiiE::Nluc assay SiiE secretion was reduced to 17.3 % of the WT level (Figure 5d).

Subsequently, the SiiE::HiBiT assay was used to investigate the effect of C26 on SiiE secretion. Treatment with different concentrations of C26 resulted in a dose dependent reduction of SiiE surface retention (Figure 6c) and secretion (Figure

6d). SiiE expression was further analysed on the SDS-PAGE (Figure 6e). It must be clearly stated that the used 4 - 20 % SDS-PAGE is not suitable for electrophoresis of a 595 kDa protein. Other authors used 1.3 % agarose gels and phosphate buffer systems for immunodetection of SiiE (Gerlach et al. 2007b). SiiE was also separated on NuPAGE Tris-Acetate gels (Kiss et al. 2007; Main-Hester et al. 2008). However, the SDS-PAGE analysis used herein confirmed that C26 also inhibits expression and not only the secretion of SiiE. In contrast, in the SiiF G500E and Δ*siiF* mutant strains SiiE secretion but not its expression was impaired (Figure 6e), which is in line with previous findings (Gerlach et al. 2007b; Kiss et al. 2007; Morgan et al. 2007; Main-Hester et al. 2008; Gerlach et al. 2009).

The HiBiT tag was also used to detect SiiE in crude membranes on the BN-PAGE (Figure 6f), as it was not clear whether SiiE could be present in the upper 900 kDa band (Figure 4a). Wagner et al. suggested that SiiE could be retained temporarily inside the T1SS channel (Wagner 2011; Wagner et al. 2011). SiiF G500E and K506L mutant strains were used as negative controls, as they most likely fail to assemble the T1SS (Figure 4c). In all tested SiiE::HiBiT mutants a weak band located above 1200 kDa was observed (Figure 6f). Therefore it can be concluded that SiiE is not associated with the 900 kDa membrane protein complex. It is most likely that residual SiiE from the cytosol or supernatant is responsible for the small 1200 kDa bands.

In addition to the SiiE::HiBiT end point assay, *Salmonella* strains were grown in a 96-well plate and SiiE secretion was assessed every 5 min with a kinetic measurement (Figure 7). It was reported that maximal SiiE secretion and surface retention occur in the late exponential growth phase after 3.5 h of subculture (Wagner et al. 2011). When subcultured in the 96-well plate, maximal SiiE secretion was observed already after 2 - 3 h corresponding to mid-exponential growth phase. It is worth noting that bacteria were subcultured to a target $OD_{600}$ of 0.1 instead of 0.05, like for the other subcultures used in this study. Before subculturing, bacterial cells were also washed twice in PBS to remove all

previously secreted SiiE. This procedure can further influence bacterial growth. Although the Tecan plate reader was prewarmed to 37°C, aeration and shaking are different from those in the incubator. Taken together, this method includes multiple factors that can affect bacterial growth and thus protein expression. This may explain why high variations of the point in time at which SiiE secretion reached its maximum were observed in the various experiments performed (data not shown). However, the effect of C26 was reproducible with an activity observed starting from 30 min after treatment.

## 4.4 C26 reduces host cell invasion

Gerlach et al. was the first to show that SiiE mediates adhesion of *Salmonella* to polarised monolayers of MDCK, CaCo-2 or T-84 cells (Gerlach et al. 2007b). SiiE mediated adhesion to polarised cells is required for efficient host cell invasion (Gerlach et al. 2008).
Unexpectedly, invasion of MDCK cells was not reduced in the ΔSPI4 or Δ*siiF* mutant strains compared to the WT level (Figure 9b). This unforeseen result suggests that the MDCK cells were most likely not properly polarised. Hence, under the experimental conditions used in this study, conclusions can only be drawn about the effect of C26 on T3SS-1 mediated invasion of MDCK cells but not on additional inhibition of SPI-4 mediated adhesion (Gerlach et al. 2008).

However, in presence of 100 µM of C26, invasion of HeLa cells was reduced to 36.9 % and invasion of MDCK cells was reduced to 49.2 % of the non-treated WT level (Figure 9).
Beside C26 there are currently other compounds under investigation targeting the T3SS-1 and also preventing *Salmonella* invasion of mammalian host cells (reviewed in Hussain et al. 2021).

Recently, a small molecule targeting the transcriptional regulator of T3SS-1 effector protein expression InvF in *S*. Typhimurium was described (Boonyom et al. 2022). At a concentration of 100 µM this compound inhibits SipA and SipC secretion and reduces invasion of HT29 cells by approximately 50 % compared

to WT level (Boonyom et al. 2022). C26 led to a similar reduction of invasion capacity (Figure 9).

Wu et al. investigated a natural compound from the medicinal plant *Myrica nagi* that, similarly to C26, targets the transcriptional regulator HilD. Myricanol binds HilD, reduces its DNA-binding activity and thereby inhibits *hilA* and *invF* gene expression (Wu et al. 2020). At a concentration of 100 µM Myricanol inhibits SPI-1 effector protein secretion and reduces invasion of SW480 cells by more than 90 % (Wu et al. 2020). Elucidation of the crystal structure of HilD will be crucial to compare the binding properties of C26 or Myricanol to HilD (Wu et al. 2020) and to possibly design more potent C26 derivatives (Abdelhakim Boudrioua, personal communication 2021).

Another natural compound and SPI-1 inhibitor is syringaldehyde, which is obtained from the stems of *Hibiscus taiwanesis*. It reduces transcription of *hilD*, *hilC*, *rtsA*, *invF*, *hilA*, *sipA*, *sipB* and *sipC* genes (Lv et al. 2019). Invasion of HeLa cells was reduced by approximately 40 % in presence of 0.18 mM syringaldehyde compared to non-treated WT strain (Lv et al. 2019).

Lastly, the generation of polarised MDCK cell monolayers (Gerlach et al. 2007b) is discussed briefly. In this work the parental cell line MDCK (NBL-2) was used to generate a polarised cell monolayer (Gerlach et al. 2007b). The protocol for the MDCK cell invasion assay was adapted from previous reports (Gerlach et al. 2007b; Gerlach et al. 2008; Wagner et al. 2011; Wagner et al. 2014; Wille et al. 2014). MDCK cells were grown for 5 - 6 days (Wagner et al. 2011; Wagner et al. 2014; Wille et al. 2014) and cell confluency was followed using an inverted microscope. However, other authors reported that MDCK cells were grown for 4 - 14 days (Gerlach et al. 2007b) or 6 - 10 days (Gerlach et al. 2008). In this study, no further methods allowing control of the cell polarisation process like TEER (transepithelial electrical resistance) were used. TEER can also be used to show how cell-to-cell contacts get disrupted after infection with *Salmonella* (Gerlach et al. 2008). It should be noted that there are more than nine different

MDCK strains available (Dukes et al. 2011). It cannot be ruled out that the culture requirements of the parental MDCK (NBL-2) cell line differ from those of MDCK cells used by other authors to generate a polarised cell monolayer (Gerlach et al. 2007b; Gerlach et al. 2008; Wagner et al. 2011; Wille et al. 2014).
Gerlach et al. refer to “MDCK cells” (Gerlach et al. 2007b; Gerlach et al. 2008). Peters et al. used the “MDCK Pf subclone” (Peters et al. 2017), although this cell line is not listed in the ATCC (American Type Culture Collection) or ECACC (European Collection of Authenticated Cell Cultures). It is highly recommended to report the used strain and origin of the cells (Table 9) (Dukes et al. 2011).

Taken together, I was able to show that C26 reduced host cell invasion (Figure 9). Nonetheless, further experiments are required to quantify the effect of C26 on *Salmonella* adhesion to and invasion of monolayers of polarised epithelial cells.

## 4.5 C26 inhibits SipA-HiBiT injection

To investigate the function of SPI-4 and the effect of C26 on T3SS-1 effector protein injection I used the split HiBiT-LgBiT assay. Here the injection of SipA-HiBiT into HeLa-LgBiT cells is quantified by measuring a luminescence signal (Westerhausen et al. 2020).
Using the SipA-HiBiT injection assay I could confirm that SPI-4 is not required for T3SS-1 effector protein injection into HeLa-LgBiT cells (Figure 10). Surprisingly, though, SipA-HiBiT injection was even enhanced by 35 % in the ΔSPI4 mutant compared to the WT level.

We hypothesised that the absence of the 175 ± 5 nm long adhesin SiiE (Wagner et al. 2011) on the bacterial surface could make more space for the T3SS-1 injectisome and enhances effector protein translocation in non-polarised HeLa cells (Samuel Wagner, personal communication 2021). Increased T3SS-1 effector protein injection could explain why also slightly more bacteria invaded HeLa cells in the ΔSPI4 mutant strain (Figure 9a).

Beside investigating the role of SPI-4 for T3SS-1 function, the effect of C26 on T3SS-1 effector protein injection was quantified. C26 reduced SipA-HiBiT injection in a dose-dependent manner. In WT strains treated with 100 µM C26, SipA-HiBiT injection was reduced to approximately 5.8 % of the WT level (Figure 10). A similar reduction was observed in the SiiE::HiBiT secretion assay, where SiiE secretion was reduced to 2.6 % of the WT level in presence of 100 µM C26 (Figure 6).

Although SipA-HiBiT injection was reduced to 5.8 % of the WT level in presence of 100 µM C26, the invasion of HeLa cells and MDCK cells was reduced to a lesser extent, that is, to 36.9 % and 49.2 % of the WT level, respectively (Figure 9). These findings suggest that the residual T3SS-1 function is sufficient to mediate invasion of a subgroup of *Salmonella* into non-polarised HeLa cells and most likely into non-polarised MDCK cells. In the Δ*hilD* negative control only 0.08 % SipA-HiBiT was injected into HeLa-LgBiT cells as compared to the WT level (Figure 10) and the invasion of HeLa cells was reduced to 0.03 % of the WT level (Figure 9a).

We speculate that in the ΔSPI4 mutant strain SipA-HiBiT injection into polarised cells is strongly reduced. Further work needs to be done to establish polarised epithelial cells stably expressing LgBiT to quantify the function of SPI-4 for T3SS-1 effector protein injection into polarised cell monolayers.

# 5 Summary

The lab of Samuel Wagner has been developing the small molecule called Compound 26 (C26) as an anti-virulence agent against infections with the bacterial enteropathogen *Salmonella* Typhimurium. C26 targets the main transcriptional regulator of *Salmonella* pathogenicity HilD (Abdelhakim Boudrioua, personal communication 2021).

In this work, the effect of C26 on *Salmonella* pathogenicity island 4 (SPI-4) and the giant non-fimbrial adhesin SiiE was investigated.
In particular, analysis of the expression and assembly of the SPI-4 encoded T1SS via SDS-PAGE and BN-PAGE revealed that 100 µM C26 strongly reduced the expression of the T1SS ABC-transporter, SiiF, and impeded the assembly of this secretion system. The establishment of a HiBiT-LgBiT based SiiE secretion assay enabled the quantification of SiiE secretion into the culture medium. T3SS-1 dependent injection of SipA-HiBiT into HeLa-LgBiT cells was assessed using the previously established injection assay (Westerhausen et al. 2020). Using these assays, I was able to show that C26 reduced SiiE secretion and SipA-HiBiT injection in a dose-dependent manner. At concentrations of 100 µM C26 SiiE secretion was reduced to 2.6 % of the wild type level and SipA-HiBiT injection into HeLa-LgBiT cells was reduced to 5.6 % of the wild type level.
As evidenced by an *in vitro* cell invasion assay, C26 reduced invasion of *Salmonella* into non-polarised HeLa and MDCK cells. Unfortunately, it was not possible to generate polarised monolayers of MDCK cells, which are a prerequisite for quantifying SPI-4 mediated adhesion to polarised epithelial cells (Gerlach et al. 2007b).

In conclusion, this work showed that C26 reduced SiiF expression, T1SS assembly, SiiE secretion and attenuated the invasion capacity of *Salmonella* into host cells. Together, these findings strengthen the role of C26 as a promising new candidate for antimicrobial therapy.

# 6 Deutsche Zusammenfassung

Das Labor von Samuel Wagner hat das kleine Molekül Compound 26 (C26) als ein Anti-Virulenz-Mittel gegen Infektionen mit dem enteropathogenen *Salmonella* Typhimurium entwickelt. C26 zielt auf den Haupttranskriptionsfaktor für die *Salmonella* Pathogenität HilD (Abdelhakim Boudrioua, persönliche Kommunikation 2021).

In dieser Arbeit wurde die Wirkung von C26 auf die *Salmonella* Pathogenitätsinsel 4 (SPI-4) und das große nicht-fimbrilläre Adhäsin SiiE untersucht. Die Analyse der Expression und des Zusammenbaus des SPI-4 kodierten T1SS mittels SDS-PAGE und BN-PAGE ergab insbesondere, dass 100 µM C26 die Expression des T1SS ABC-Transporters SiiF deutlich reduzierte und den Zusammenbau dieses Sekretionssystems verhinderte. Die Etablierung eines HiBiT-LgBiT basierten SiiE Sekretions-Assays ermöglichte die Quantifizierung der SiiE Sekretion in das Kulturmedium. Die T3SS-1 abhängige Injektion von SipA-HiBiT in HeLa-LgBiT Zellen wurde mittels eines bereits früher etablierten Injektions-Assays bestimmt (Westerhausen et al. 2020). Durch die Nutzung dieser Assays konnte ich die dosisabhängige Reduktion der SiiE Sekretion und SipA Injektion durch C26 zeigen. Bei Konzentrationen von 100 µM C26 war die Sekretion von SiiE auf 2.6 % des Wildtyp-Werts und die Injektion von SipA-HiBiT in HeLa-LgBiT Zellen auf 5.6 % des Wildtyp-Werts reduziert. In einem *in vitro* Zellinvasions-Assay wurde gezeigt, dass C26 die Invasion von *Salmonella* in nicht polarisierte HeLa und MDCK Zellen reduzierte. Leider war es nicht möglich, polarisierte Monolayer von MDCK Zellen zu erzeugen, welche eine Voraussetzung für die Bestimmung der SPI-4 vermittelten Adhäsion an polarisierte Epithelzellen sind (Gerlach et al. 2007b).
Zusammenfassend zeigt diese Arbeit, dass C26 die Expression von SiiF, den T1SS Zusammenbau, die Sekretion von SiiE reduzierte und die Invasionskapazität von *Salmonella* in Wirtszellen abschwächte. Gemeinsam heben diese Ergebnisse die Rolle von C26 als einen vielversprechenden neuen Kandidaten für die antimikrobielle Therapie hervor.

# 7 Literature


Agilent Technologies QuikChange Site-Directed Mutagenesis Kit: Instruction Manual. https://www.agilent.com/cs/library/usermanuals/Public/200518.pdf. Accessed May 26, 2022

Ahmer, B. M. M.; van Reeuwijk, J.; Watson, P. R.; Wallis, T. S. and Heffron, F. (1999). Salmonella SirA is a global regulator of genes mediating enteropathogenesis. *Mol Microbiol.* **31**(3):971-982. https://doi.org/10.1046/j.1365-2958.1999.01244.x

Alav, I.; Kobylka, J.; Kuth, M. S.; Pos, K. M.; Picard, M.; Blair, J. M. A. and Bavro, V. N. (2021). Structure, Assembly, and Function of Tripartite Efflux and Type 1 Secretion Systems in Gram-Negative Bacteria. *Chem Rev.* **121**(9):5479-5596. https://doi.org/10.1021/acs.chemrev.1c00055

Bajaj, V.; Lucas, R. L.; Hwang, C. and Lee, C. A. (1996). Co-ordinate regulation of Salmonella typhimurium invasion genes by environmental and regulatory factors is mediated by control of hilA expression. *Mol Microbiol.* **22**(4):703-714. https://doi.org/10.1046/j.1365-2958.1996.d01-1718.x

Barlag, B. and Hensel, M. (2015). The Giant Adhesin SiiE of Salmonella enterica. *Molecules* **20**(1):1134-1150. https://doi.org/10.3390/molecules20011134

Baxter, M. A. and Jones, B. D. (2015). Two-Component Regulators Control hilA Expression by Controlling fimZ and hilE Expression within Salmonella enterica Serovar Typhimurium. *Infect Immun* **83**(3):978-985. https://doi.org/10.1128/IAI.02506-14

Beer, T. (2020). Isolation and cellular characterization of the hemolysin A type 1 secretion system from Escherichia coli. Dissertation. Heinrich-Heine-Universität, Düsseldorf. urn:nbn:de:hbz:061-20200716-105128-1

Boonyom, R.; Roytrakul, S. and Thinwang, P. (2022). A small molecule, C24H17ClN4O2S, inhibits the function of the type III secretion system in Salmonella Typhimurium. *J Genet Eng Biotechnol.* **20**(1):54. https://doi.org/10.1186/s43141-022-00336-1

CDC (2019). Antibiotic Resistance Threats in the United States, 2019, Atlanta, GA: U.S. Department of Health and Human Services. https://www.cdc.gov/drugresistance/pdf/threats-report/2019-ar-threats-report-508.pdf. Accessed May 26, 2022

CDC (2021). Salmonella: Salmonella Homepage. https://www.cdc.gov/salmonella/index.html. Accessed May 26, 2022

Cegelski, L.; Marshall, G. R.; Eldridge, G. R. and Hultgren, S. J. (2008). The biology and future prospects of antivirulence therapies. *Nat Rev Microbiol.* **6**(1):17-27. https://doi.org/10.1038/nrmicro1818

Chlebicz, A. and Śliżewska, K. (2018). Campylobacteriosis, Salmonellosis, Yersiniosis, and Listeriosis as Zoonotic Foodborne Diseases: A Review. *Int. J. Environ. Res. Public Health* **15**(5):863. https://doi.org/10.3390/ijerph15050863

Costa, T. R. D.; Felisberto-Rodrigues, C.; Meir, A.; Prevost, M. S.; Redzej, A.; Trokter, M. and Waksman, G. (2015). Secretion systems in Gram-negative bacteria: structural and mechanistic insights. *Nat Rev Microbiol.* **13**(6):343-359. https://doi.org/10.1038/nrmicro3456

De Keersmaecker, S. C. J.; Marchal, K.; Verhoeven, T. L. A.; Engelen, K.; Vanderleyden, J. and Detweiler, C. S. (2005). Microarray analysis and motif detection reveal new targets of the Salmonella enterica serovar Typhimurium HilA regulatory protein, including hilA itself. *Journal of bacteriology* **187**(13):4381-4391. https://doi.org/10.1128/JB.187.13.4381-4391.2005

Deng, W.; Marshall, N. C.; Rowland, J. L.; McCoy, J. M.; Worrall, L. J.; Santos, A. S.; Strynadka, N. C. J. and Finlay, B. B. (2017). Assembly, structure, function and regulation of type III secretion systems. *Nat Rev Microbiol.* **15**(6):323-337. https://doi.org/10.1038/nrmicro.2017.20

Dukes, J. D.; Whitley, P. and Chalmers, A. D. (2011). The MDCK variety pack: choosing the right strain. *BMC Cell Biol.* **12**:43. https://doi.org/10.1186/1471-2121-12-43

Ellermeier, C. D.; Ellermeier, J. R. and Slauch, J. M. (2005). HilD, HilC and RtsA constitute a feed forward loop that controls expression of the SPI1 type three secretion system regulator hilA in Salmonella enterica serovar Typhimurium. *Mol Microbiol.* **57**(3):691-705. https://doi.org/10.1111/j.1365-2958.2005.04737.x

Ellermeier, C. D. and Slauch, J. M. (2003). RtsA and RtsB coordinately regulate expression of the invasion and flagellar genes in Salmonella enterica serovar Typhimurium. *J Bacteriol.* **185**(17):5096-5108. https://doi.org/10.1128/JB.185.17.5096-5108.2003

Ellermeier, J. R. and Slauch, J. M. (2007). Adaptation to the host environment: regulation of the SPI1 type III secretion system in Salmonella enterica serovar Typhimurium. *Curr Opin Microbiol.* **10**(1):24-29. https://doi.org/10.1016/j.mib.2006.12.002

England, C. G.; Ehlerding, E. B. and Cai, W. (2016). NanoLuc: A Small Luciferase Is Brightening Up the Field of Bioluminescence. *Bioconjug Chem.* **27**(5):1175-1187. https://doi.org/10.1021/acs.bioconjchem.6b00112

Fàbrega, A. and Vila, J. (2013). Salmonella enterica serovar Typhimurium skills to succeed in the host: virulence and regulation. *Clin Microbiol Rev.* **26**(2):308-341. https://doi.org/10.1128/CMR.00066-12

García Véscovi, E.; Soncini, F. C. and Groisman, E. A. (1996). Mg2+ as an Extracellular Signal: Environmental Regulation of Salmonella Virulence. *Cell* **84**(1):165-174. https://doi.org/10.1016/S0092-8674(00)81003-X

Gerlach, R. G.; Cláudio, N.; Rohde, M.; Jäckel, D.; Wagner, C. and Hensel, M. (2008). Cooperation of Salmonella pathogenicity islands 1 and 4 is required to breach epithelial barriers. *Cell Microbiol* **10**(11):2364-2376. https://doi.org/10.1111/j.1462-5822.2008.01218.x

Gerlach, R. G. and Hensel, M. (2007). Protein secretion systems and adhesins: The molecular armory of Gram-negative pathogens. *Int J Med Microbiol.* **297**(6):401-415. https://doi.org/10.1016/j.ijmm.2007.03.017

Gerlach, R. G.; Jäckel, D.; Geymeier, N. and Hensel, M. (2007a). Salmonella pathogenicity island 4-mediated adhesion is coregulated with invasion genes in Salmonella enterica. *Infect Immun.* **75**(10):4697-4709. https://doi.org/10.1128/IAI.00228-07

Gerlach, R. G.; Jäckel, D.; Hölzer, S. U. and Hensel, M. (2009). Rapid oligonucleotide-based recombineering of the chromosome of Salmonella enterica. *Appl. Environ. Microbiol.* **75**(6):1575-1580. https://doi.org/10.1128/AEM.02509-08

Gerlach, R. G.; Jäckel, D.; Stecher, B.; Wagner, C.; Lupas, A.; Hardt, W.-D. and Hensel, M. (2007b). Salmonella Pathogenicity Island 4 encodes a giant non-fimbrial adhesin and the cognate type 1 secretion system. *Cell Microbiol* **9**(7):1834-1850. https://doi.org/10.1111/j.1462-5822.2007.00919.x

Geymeier, N. (2011). Das große nicht-fimbrilläre Adhäsin SiiE von Salmonella enterica: Untersuchungen zur Verbreitung, Regulation und Sekretion. Dissertation. Friedrich-Alexander-Universität, Erlangen-Nürnberg. urn:nbn:de:bvb:29-opus-25153

Gibson, D. G.; Young, L.; Chuang, R.-Y.; Venter, J. C.; Hutchison 3rd, C. A. and Smith, H. O. (2009). Enzymatic assembly of DNA molecules up to several hundred kilobases. *Nat Methods* **6**(5):343-345. https://doi.org/10.1038/nmeth.1318

Golubeva, Y. A.; Sadik, A. Y.; Ellermeier, J. R. and Slauch, J. M. (2012). Integrating global regulatory input into the Salmonella pathogenicity island 1 type III secretion system. *Genetics* **190**(1):79-90. https://doi.org/10.1534/genetics.111.132779

Grenz, J. R.; Cott Chubiz, J. E.; Thaprawat, P. and Slauch, J. M. (2018). HilE Regulates HilD by Blocking DNA Binding in Salmonella enterica Serovar Typhimurium. *J Bacteriol.* **200**(8):e00750-17. https://doi.org/10.1128/JB.00750-17

Groisman, E. A. (2001). The pleiotropic two-component regulatory system PhoP-PhoQ. *J Bacteriol.* **183**(6):1835-1842. https://doi.org/10.1128/JB.183.6.1835-1842.2001

Hansmeier, N.; Miskiewicz, K.; Elpers, L.; Liss, V.; Hensel, M. and Sterzenbach, T. (2017). Functional expression of the entire adhesiome of Salmonella enterica serotype Typhimurium. *Sci Rep* **7**(1):10326. https://doi.org/10.1038/s41598-017-10598-2

Hensel, M. (2000). Salmonella pathogenicity island 2. *Mol Microbiol.* **36**(5):1015-1023. https://doi.org/10.1046/j.1365-2958.2000.01935.x

Hotinger, J. A.; Pendergrass, H. A. and May, A. E. (2021). Molecular Targets and Strategies for Inhibition of the Bacterial Type III Secretion System (T3SS); Inhibitors Directly Binding to T3SS Components. *Biomolecules* **11**(2):316. https://doi.org/10.3390/biom11020316

Hurley, A. (2018). Old Reliable: Two-Step Allelic Exchange. https://bitesizebio.com/41461/old-reliable-two-step-allelic-exchange/. Accessed May 26, 2022

Hussain, S.; Ouyang, P.; Zhu, Y.; Khalique, A.; He, C.; Liang, X.; Shu, G. and Yin, L. (2021). Type 3 secretion system 1 of Salmonella typhimurium and its inhibitors: a novel strategy to combat salmonellosis. *Environ Sci Pollut Res Int.* **28**(26):34154-34166. https://doi.org/10.1007/s11356-021-13986-4

Ibarra, J. A.; Knodler, L. A.; Sturdevant, D. E.; Virtaneva, K.; Carmody, A. B.; Fischer, E. R.; Porcella, S. F. and Steele-Mortimer, O. (2010). Induction of Salmonella pathogenicity island 1 under different growth conditions can affect Salmonella-host cell interactions in vitro. *Microbiology* **156**(Pt 4):1120-1133. https://doi.org/10.1099/mic.0.032896-0

Jajere, S. M. (2019). A review of Salmonella enterica with particular focus on the pathogenicity and virulence factors, host specificity and antimicrobial resistance including multidrug resistance. *Vet World.* **12**(4):504-521. https://doi.org/10.14202/vetworld.2019.504-521

Jo, I.; Kim, J.-S.; Xu, Y.; Hyun, J.; Lee, K. and Ha, N.-C. (2019). Recent paradigm shift in the assembly of bacterial tripartite efflux pumps and the type I secretion system. *J Microbiol.* **57**(3):185-194. https://doi.org/10.1007/s12275-019-8520-1

Kalafatis, M. and Slauch, J. M. (2021). Long-Distance Effects of H-NS Binding in the Control of hilD Expression in the Salmonella SPI1 Locus. *Journal of bacteriology* **203**(21):e0030821. https://doi.org/10.1128/JB.00308-21

Kanonenberg, K.; Spitz, O.; Erenburg, I. N.; Beer, T. and Schmitt, L. (2018). Type I secretion system-it takes three and a substrate. *FEMS Microbiol Lett.* **365**(11). https://doi.org/10.1093/femsle/fny094

Kim, K.; Palmer, A. D.; Vanderpool, C. K. and Slauch, J. M. (2019). The Small RNA PinT Contributes to PhoP-Mediated Regulation of the Salmonella Pathogenicity Island 1 Type III Secretion System in Salmonella enterica Serovar Typhimurium. *Journal of bacteriology* **201**(19):e00312-19. https://doi.org/10.1128/JB.00312-19

Kirchweger, P.; Weiler, S.; Egerer-Sieber, C.; Blasl, A.-T.; Hoffmann, S.; Schmidt, C.; Sander, N.; Merker, D.; Gerlach, R. G.; Hensel, M. and Muller, Y. A. (2019). Structural and functional characterization of SiiA, an auxiliary protein from the SPI4-encoded type 1 secretion system from Salmonella enterica. *Mol Microbiol.* **112**(5):1403-1422. https://doi.org/10.1111/mmi.14368

Kiss, T.; Morgan, E. and Nagy, G. (2007). Contribution of SPI-4 genes to the virulence of Salmonella enterica. *FEMS Microbiol Lett.* **275**(1):153-159. https://doi.org/10.1111/j.1574-6968.2007.00871.x

Klingl, S.; Kordes, S.; Schmid, B.; Gerlach, R. G.; Hensel, M. and Muller, Y. A. (2020). Recombinant protein production and purification of SiiD, SiiE and SiiF - Components of the SPI4-encoded type I secretion system from Salmonella Typhimurium. *Protein Expr Purif.* **172**:105632. https://doi.org/10.1016/j.pep.2020.105632

Lee, J. (2017). HiBiT: A Tiny Tag for Antibody-Free Endogenous Protein Detection. https://www.promega.de/resources/pubhub/features/hibit-a-tiny-tag-for-antibody-free-endogenous-protein-detection/. Accessed May 26, 2021

Lenders, M. H. H. (2015). Mechanisms of hemolysin A Type 1 secretion in Escherichia coli. Dissertation. Heinrich-Heine-Universität, Düsseldorf. urn:nbn:de:hbz:061-20160114-100840-3

Li, X.; Bleumink-Pluym, N. M. C.; Luijkx, Y. M. C. A.; Wubbolts, R. W.; van Putten, J. P. M. and Strijbis, K. (2019). MUC1 is a receptor for the Salmonella SiiE adhesin that enables

apical invasion into enterocytes. *PLoS Pathog* **15**(2):e1007566. https://doi.org/10.1371/journal.ppat.1007566

Lou, L.; Zhang, P.; Piao, R. and Wang, Y. (2019). Salmonella Pathogenicity Island 1 (SPI-1) and Its Complex Regulatory Network. *Front. Cell. Infect. Microbiol.* **9**:270. https://doi.org/10.3389/fcimb.2019.00270

Lucchini, S.; Rowley, G.; Goldberg, M. D.; Hurd, D.; Harrison, M. and Hinton, J. C. D. (2006). H-NS mediates the silencing of laterally acquired genes in bacteria. *PLoS Pathog* **2**(8):e81. https://doi.org/10.1371/journal.ppat.0020081

Lv, Q.; Chu, X.; Yao, X.; Ma, K.; Zhang, Y. and Deng, X. (2019). Inhibition of the type III secretion system by syringaldehyde protects mice from Salmonella enterica serovar Typhimurium. *J Cell Mol Med.* **23**(7):4679-4688. https://doi.org/10.1111/jcmm.14354

Main-Hester, K. L.; Colpitts, K. M.; Thomas, G. A.; Fang, F. C. and Libby, S. J. (2008). Coordinate Regulation of Salmonella Pathogenicity Island 1 (SPI1) and SPI4 in Salmonella enterica Serovar Typhimurium. *Infect Immun.* **76**(3):1024-1035. https://doi.org/10.1128/IAI.01224-07

Majowicz, S. E.; Musto, J.; Scallan, E.; Angulo, F. J.; Kirk, M.; O'Brien, S. J.; Jones, T. F.; Fazil, A. and Hoekstra, R. M. (2010). The global burden of nontyphoidal Salmonella gastroenteritis. *Clin Infect Dis.* **50**(6):882-889. https://doi.org/10.1086/650733

Martínez, L. C.; Yakhnin, H.; Camacho, M. I.; Georgellis, D.; Babitzke, P.; Puente, J. L. and Bustamante, V. H. (2011). Integration of a complex regulatory cascade involving the SirA/BarA and Csr global regulatory systems that controls expression of the Salmonella SPI-1 and SPI-2 virulence regulons through HilD. *Mol Microbiol.* **80**(6):1637-1656. https://doi.org/10.1111/j.1365-2958.2011.07674.x

McClelland, M.; Sanderson, K. E.; Spieth, J.; Clifton, S. W.; Latreille, P.; Courtney, L.; Porwollik, S.; Ali, J.; Dante, M.; Du, F.; Hou, S.; Layman, D.; Leonard, S.; Nguyen, C.; Scott, K.; Holmes, A.; Grewal, N.; Mulvaney, E.; Ryan, E.; Sun, H.; Florea, L.; Miller, W.; Stoneking, T.; Nhan, M.; Waterston, R. and Wilson, R. K. (2001). Complete genome sequence of Salmonella enterica serovar Typhimurium LT2. *Nature* **413**(6858):852-856. https://doi.org/10.1038/35101614

Morgan, E.; Bowen, A. J.; Carnell, S. C.; Wallis, T. S. and Stevens, M. P. (2007). SiiE is secreted by the Salmonella enterica serovar Typhimurium pathogenicity island 4-encoded secretion system and contributes to intestinal colonization in cattle. *Infect Immun* **75**(3):1524-1533. https://doi.org/10.1128/IAI.01438-06

Morgan, E.; Campbell, J. D.; Rowe, S. C.; Bispham, J.; Stevens, M. P.; Bowen, A. J.; Barrow, P. A.; Maskell, D. J. and Wallis, T. S. (2004). Identification of host-specific colonization factors of Salmonella enterica serovar Typhimurium. *Mol Microbiol.* **54**(4):994-1010. https://doi.org/10.1111/j.1365-2958.2004.04323.x

Nair, D. V. T.; Venkitanarayanan, K. and Kollanoor Johny, A. (2018). Antibiotic-Resistant Salmonella in the Food Supply and the Potential Role of Antibiotic Alternatives for Control. *Foods* **7**(10):167. https://doi.org/10.3390/foods7100167

Narm, K.-E.; Kalafatis, M. and Slauch, J. M. (2020). HilD, HilC, and RtsA Form Homodimers and Heterodimers To Regulate Expression of the Salmonella Pathogenicity Island I Type III Secretion System. *J Bacteriol.* **202**(9):e00012-20. https://doi.org/10.1128/JB.00012-20

Navarre, W. W.; McClelland, M.; Libby, S. J. and Fang, F. C. (2007). Silencing of xenogeneic DNA by H-NS-facilitation of lateral gene transfer in bacteria by a defense system that recognizes foreign DNA. *Genes & development* **21**(12):1456-1471. https://doi.org/10.1101/gad.1543107

Palmer, A. D.; Kim, K. and Slauch, J. M. (2019). PhoP-Mediated Repression of the SPI1 Type 3 Secretion System in Salmonella enterica Serovar Typhimurium. *J Bacteriol.* **201**(16):e00264-19. https://doi.org/10.1128/JB.00264-19

Paredes-Amaya, C. C.; Valdés-García, G.; Juárez-González, V. R.; Rudiño-Piñera, E. and Bustamante, V. H. (2018). The Hcp-like protein HilE inhibits homodimerization and DNA binding of the virulence-associated transcriptional regulator HilD in Salmonella. *J Biol Chem.* **293**(17):6578-6592. https://doi.org/10.1074/jbc.RA117.001421

Pérez-Morales, D.; Nava-Galeana, J.; Rosales-Reyes, R.; Teehan, P.; Yakhnin, H.; Melchy-Pérez, E. I.; Rosenstein, Y.; De La Cruz, M. A.; Babitzke, P. and Bustamante, V. H. (2021). An incoherent feedforward loop formed by SirA/BarA, HilE and HilD is involved in controlling the growth cost of virulence factor expression by Salmonella Typhimurium. *PLoS Pathog* **17**(5):e1009630. https://doi.org/10.1371/journal.ppat.1009630

Peters, B.; Stein, J.; Klingl, S.; Sander, N.; Sandmann, A.; Taccardi, N.; Sticht, H.; Gerlach, R. G.; Muller, Y. A. and Hensel, M. (2017). Structural and functional dissection reveals distinct roles of Ca2+-binding sites in the giant adhesin SiiE of Salmonella enterica. *PLoS Pathog* **13**(5):e1006418. https://doi.org/10.1371/journal.ppat.1006418

Petrone, B. L.; Stringer, A. M. and Wade, J. T. (2014). Identification of HilD-regulated genes in Salmonella enterica serovar Typhimurium. *J Bacteriol.* **196**(5):1094-1101. https://doi.org/10.1128/JB.01449-13

Rehman, T.; Yin, L.; Latif, M. B.; Chen, J.; Wang, K.; Geng, Y.; Huang, X.; Abaidullah, M.; Guo, H. and Ouyang, P. (2019). Adhesive mechanism of different Salmonella fimbrial adhesins. *Microb Pathog.* **137**:103748. https://doi.org/10.1016/j.micpath.2019.103748

RKI (2008). RKI - RKI-Ratgeber - Typhus abdominalis, Paratyphus. https://www.rki.de/DE/Content/Infekt/EpidBull/Merkblaetter/Ratgeber_Typhus_Paratyphus.html;jsessionid=017114572C210EDFAA75EC58B17BFA6F.internet101. Accessed May 26, 2022

RKI (2016). Salmonellose: RKI-Ratgeber. https://www.rki.de/DE/Content/Infekt/EpidBull/Merkblaetter/Ratgeber_Salmonellose.html. Accessed May 26, 2022

Ryan, M. P.; O'Dwyer, J. and Adley, C. C. (2017). Evaluation of the Complex Nomenclature of the Clinically and Veterinary Significant Pathogen Salmonella. *Biomed Res Int.* **2017**:3782182. https://doi.org/10.1155/2017/3782182

S2k-Leitlinie (2015). Gastrointestinale Infektionen und Morbus Whipple: AWMF-Register-Nr. 021/024 Klasse S2k. https://www.awmf.org/leitlinien/detail/ll/021-024.html. Accessed May 26, 2022

Saini, S.; Ellermeier, J. R.; Slauch, J. M. and Rao, C. V. (2010). The role of coupled positive feedback in the expression of the SPI1 type three secretion system in Salmonella. *PLoS Pathog* **6**(7):e1001025. https://doi.org/10.1371/journal.ppat.1001025

Saini, S. and Rao, C. V. (2010). SprB is the molecular link between Salmonella pathogenicity island 1 (SPI1) and SPI4. *J Bacteriol.* **192**(9):2459-2462. https://doi.org/10.1128/JB.00047-10

Schägger, H. and von Jagow, G. (1991). Blue native electrophoresis for isolation of membrane protein complexes in enzymatically active form. *Anal Biochem.* **199**(2):223-231. https://doi.org/10.1016/0003-2697(91)90094-A

Schwinn, M. K.; Machleidt, T.; Zimmerman, K.; Eggers, C. T.; Dixon, A. S.; Hurst, R.; Hall, M. P.; Encell, L. P.; Binkowski, B. F. and Wood, K. V. (2018). CRISPR-Mediated Tagging of Endogenous Proteins with a Luminescent Peptide. *ACS chemical biology* **13**(2):467-474. https://doi.org/10.1021/acschembio.7b00549

Smith, C.; Stringer, A. M.; Mao, C.; Palumbo, M. J. and Wade, J. T. (2016). Mapping the Regulatory Network for Salmonella enterica Serovar Typhimurium Invasion. *mBio* **7**(5):e01024-16. https://doi.org/10.1128/mBio.01024-16

Spitz, O.; Erenburg, I. N.; Beer, T.; Kanonenberg, K.; Holland, I. B. and Schmitt, L. (2019). Type I Secretion Systems-One Mechanism for All? *Microbiol Spectr.* **7**(2). https://doi.org/10.1128/microbiolspec.PSIB-0003-2018

Tang, L. (2019). Investigating heterogeneity in HeLa cells. *Nat Methods* **16**(4):281. https://doi.org/10.1038/s41592-019-0375-1

Thijs, I. M. V.; De Keersmaecker, S. C. J.; Fadda, A.; Engelen, K.; Zhao, H.; McClelland, M.; Marchal, K. and Vanderleyden, J. (2007). Delineation of the Salmonella enterica serovar Typhimurium HilA regulon through genome-wide location and transcript analysis. *J Bacteriol.* **189**(13):4587-4596. https://doi.org/10.1128/JB.00178-07

Wagner, C. (2011). Characterisation of the Salmonella Pathogenicity Island 4-encoded proteins SiiE, SiiA and SiiB: a new mechanism of bacterial adhesion. Dissertation. Friedrich-Alexander-Universität, Erlangen-Nürnberg. urn:nbn:de:bvb:29-opus-25064

Wagner, C.; Barlag, B.; Gerlach, R. G.; Deiwick, J. and Hensel, M. (2014). The Salmonella enterica giant adhesin SiiE binds to polarized epithelial cells in a lectin-like manner. *Cell Microbiol.* **16**(6):962-975. https://doi.org/10.1111/cmi.12253

Wagner, C.; Polke, M.; Gerlach, R. G.; Linke, D.; Stierhof, Y.-D.; Schwarz, H. and Hensel, M. (2011). Functional dissection of SiiE, a giant non-fimbrial adhesin of Salmonella enterica. *Cell Microbiol.* **13**(8):1286-1301. https://doi.org/10.1111/j.1462-5822.2011.01621.x

Wagner, S.; Grin, I.; Malmsheimer, S.; Singh, N.; Torres-Vargas, C. E. and Westerhausen, S. (2018). Bacterial type III secretion systems: a complex device for the delivery of bacterial effector proteins into eukaryotic host cells. *FEMS Microbiol Lett.* **365**(19):fny201. https://doi.org/10.1093/femsle/fny201

Wang, C.-H.; Hsieh, Y.-H.; Powers, Z. M. and Kao, C.-Y. (2020). Defeating Antibiotic-Resistant Bacteria: Exploring Alternative Therapies for a Post-Antibiotic Era. *Int J Mol Sci.* **21**(3):1061. https://doi.org/10.3390/ijms21031061

Westerhausen, S.; Nowak, M.; Torres-Vargas, C. E.; Bilitewski, U.; Bohn, E.; Grin, I. and Wagner, S. (2020). A NanoLuc luciferase-based assay enabling the real-time analysis of protein secretion and injection by bacterial type III secretion systems. *Mol Microbiol.* **113**(6):1240-1254. https://doi.org/10.1111/mmi.14490

WHO (2018). Salmonella (non-typhoidal). https://www.who.int/news-room/fact-sheets/detail/salmonella-(non-typhoidal). Accessed May 26, 2022

WHO (2019). New report calls for urgent action to avert antimicrobial resistance crisis. https://www.who.int/news/item/29-04-2019-new-report-calls-for-urgent-action-to-avert-antimicrobial-resistance-crisis. Accessed May 26, 2022

WHO (2020). Antibiotic resistance. https://www.who.int/news-room/fact-sheets/detail/antibiotic-resistance. Accessed May 26, 2022

WHO (2021). Antimicrobial resistance. https://www.who.int/news-room/fact-sheets/detail/antimicrobial-resistance. Accessed May 26, 2022

Wille, T.; Blank, K.; Schmidt, C.; Vogt, V. and Gerlach, R. G. (2012). Gaussia princeps luciferase as a reporter for transcriptional activity, protein secretion, and protein-protein interactions in Salmonella enterica serovar typhimurium. *Appl. Environ. Microbiol.* **78**(1):250-257. https://doi.org/10.1128/AEM.06670-11

Wille, T.; Wagner, C.; Mittelstädt, W.; Blank, K.; Sommer, E.; Malengo, G.; Döhler, D.; Lange, A.; Sourjik, V.; Hensel, M. and Gerlach, R. G. (2014). SiiA and SiiB are novel type I secretion system subunits controlling SPI4-mediated adhesion of Salmonella enterica. *Cell Microbiol* **16**(2):161-178. https://doi.org/10.1111/cmi.12222

Wong, K. K.; McClelland, M.; Stillwell, L. C.; Sisk, E. C.; Thurston, S. J. and Saffer, J. D. (1998). Identification and sequence analysis of a 27-kilobase chromosomal fragment containing a Salmonella pathogenicity island located at 92 minutes on the chromosome map of Salmonella enterica serovar typhimurium LT2. *Infect Immun.* **66**(7):3365-3371. https://doi.org/10.1128/IAI.66.7.3365-3371.1998

Wu, Y.; Yang, X.; Zhang, D. and Lu, C. (2020). Myricanol Inhibits the Type III Secretion System of Salmonella enterica Serovar Typhimurium by Interfering With the DNA-Binding Activity of HilD. *Front Microbiol.* **11**:571217. https://doi.org/10.3389/fmicb.2020.571217

Zilkenat, S.; Dietsche, T.; Monjarás Feria, J. V.; Torres-Vargas, C. E.; Mebrhatu, M. T. and Wagner, S. (2017). Blue Native PAGE Analysis of Bacterial Secretion Complexes. *Methods in molecular biology (Clifton, N.J.)* **1615**:321-351. https://doi.org/10.1007/978-1-4939-7033-9_26

# 8 Erklärung zum Eigenanteil

Die Arbeit wurde im Interfakultären Institut für Mikrobiologie und Infektionsmedizin unter Betreuung von Prof. Samuel Wagner, PhD und Mentorat von Dr. Abdelhakim Boudrioua und Dr. Sara Pais durchgeführt. Die Konzeption der Studie und der Versuche erfolgte durch Prof. Samuel Wagner, PhD.

Sämtliche Versuche wurden nach Einarbeitung durch die Labormitglieder Andrea Eipper (MTA), Dr. Abdelhakim Boudrioua (Postdoc), Dr. Sara Pais (Postdoc), Dr. Iwan Grin (Postdoc), von mir eigenständig durchgeführt.

Ich versichere, das Manuskript selbstständig verfasst zu haben und keine weiteren als die von mir angegebenen Quellen verwendet zu haben.
Inhaltliche Anmerkungen zum Manuskript und die Korrektur der englischen Schrift, Grammatik, und Wortwahl erfolgten durch Dr. Abdelhakim Boudrioua, Dr. Sara Pais, Dr. Libera Lo Presti und Prof. Samuel Wagner, PhD.

Sämtliche Grafiken, wenn nicht anders vermerkt, habe ich selbst erstellt.

Tübingen, den

Alexander Kohler

# 9 Danksagung

Zunächst möchte ich allen danken, die zum erfolgreichen Abschluss meines Studiums beigetragen haben. Besonderer Dank gilt Markus Mayer für die unzähligen Wochenenden und die unglaubliche Unterstützung.

Lieber Samuel, für die Überlassung des Themas dieser Arbeit, die strukturierte und gewissenhafte Betreuung danke ich in erster Linie Dir.
Besonderer Dank gilt Hakim, meinem brother in arms, Du hast mich von Beginn an bei Tag und Nacht geduldig und mit vollem Einsatz bei meinem Projekt unterstützt und wie kein anderer zum Gelingen dieser Arbeit beigetragen. Ich danke vor allem auch Dir, Sara, für die Einarbeitung, die unermüdliche Unterstützung und Hilfestellung bei sämtlichen Versuchen in der Zellkultur. Vielen Dank Iwan für die theoretische Einarbeitung und die Unterstützung bei jeglichen Fragen.

Liebe Andrea, liebe Melanie, ich danke euch für die Hilfestellung im Laboralltag, die tägliche Unterstützung und natürlich die vertrauten Gespräche in den Pausen. Lieber Patrick, stets hilfsbereit und mit einem aufmunternden Spruch auf den Lippen, vielen Dank für die Herstellung von Hunderten von LB Platten und natürlich die kulinarische Verwöhnung.
Für die familiäre und hilfsbereite Atmosphäre möchte ich außerdem allen aus der Arbeitsgruppe Wagner und dem Institut für Mikrobiologie und Hygiene danken.

Für die finanzielle Unterstützung dieser Arbeit danke ich dem DZIF. Vielen Dank Gisela für die Koordination. Für das unermüdliche Korrekturlesen dieser Arbeit, insbesondere der englischen Schrift, danke ich Hakim, Sara und Libera.

Meiner Familie und vor allem meinen Eltern danke ich im Besonderen für die stetige Unterstützung meines Studiums und dieser Arbeit.